

UNCLASSIFIED

AD NUMBER

ADB020481

LIMITATION CHANGES

TO:

Approved for public release; distribution is unlimited.

FROM:

Distribution authorized to U.S. Gov't. agencies only; Test and Evaluation; MAR 1976. Other requests shall be referred to Air Force Avionics Lab., Wright-Patterson AFB, OH 45433.

AUTHORITY

AFAL ltr 23 Mar 1979

THIS PAGE IS UNCLASSIFIED

THIS REPORT HAS BEEN DELIMITED  
AND CLEARED FOR PUBLIC RELEASE  
UNDER DOD DIRECTIVE 5200.20 AND  
NO RESTRICTIONS ARE IMPOSED UPON  
ITS USE AND DISCLOSURE.

DISTRIBUTION STATEMENT A

APPROVED FOR PUBLIC RELEASE;  
DISTRIBUTION UNLIMITED.



AFAL-TR-76-110 ✓

AD B020481

2



# LONG LIFE Nd: YAG LASER DEVICE

**THE PERKIN-ELMER CORPORATION**  
NORWALK, CT 06856



MAY 1977

**TECHNICAL REPORT AFAL-TR-76-110**  
**FINAL REPORT FOR PERIOD 17 MARCH 1975 - 18 MARCH 1976**

Distribution is limited to U.S. Government agencies only by reason of inclusion of test and evaluation of data; applied March 1976. Other requests for this document must be referred to AFAL/DHO Wright-Patterson Air Force Base, Ohio 45433

**AU NO.** \_\_\_\_\_  
**BDC FILE COPY**

**AIR FORCE AVIONICS LABORATORY**  
**AIR FORCE WRIGHT AERONAUTICAL LABORATORIES**  
**AIR FORCE SYSTEMS COMMAND**  
**WRIGHT-PATTERSON AIR FORCE BASE, OHIO 45433**

NOTICE

When Government drawings, specifications, or other data are used for any purpose other than in connection with a definitely related Government procurement operation, the United States Government thereby incurs no responsibility nor any obligation whatsoever; and the fact that the Government may have formulated, furnished, or in any way supplied the said drawings, specifications, or other data, is not to be regarded by implication or otherwise as in any manner licensing the holder or any other person or corporation, or conveying any rights or permission to manufacture, use, or sell any patented invention that may in any way be related thereto.

This technical report has been reviewed and is approved for publication.

*Ronald F. Paulson*

Ronald F. Paulson, Project Engineer  
Electro-Optic Sources Group  
Electro-Optics Technology Branch

FOR THE COMMANDER:

*William C. Schoonover*

William C. Schoonover, Chief  
Electro-Optics Technology Branch  
Electronic Technology Division  
Air Force Avionics Laboratory

Copies of this report should not be returned unless return is required by security considerations, contractual obligations, or notice on a specific document.

UNCLASSIFIED

SECURITY CLASSIFICATION OF THIS PAGE (When Data Entered)

19 REPORT DOCUMENTATION PAGE		READ INSTRUCTIONS BEFORE COMPLETING FORM
18 1. REPORT NUMBER AFAL TR-76-110 ✓	2. GOVT ACCESSION NO.	3. RECIPIENT'S CATALOG NUMBER
6 4. TITLE (and Subtitle) LONG LIFE Nd:YAG LASER DEVICE.	7 5. TYPE OF REPORT & PERIOD COVERED FINAL REPORT. 17 March 1975 - 18 March 1976	6. PERFORMING ORG. REPORT NUMBER REPORT NO. 12985
10 7. AUTHOR(s) DAVID A. HUCHITAL	15 8. CONTRACT OR GRANT NUMBER(s) F33615-75-C-1193	
9. PERFORMING ORGANIZATION NAME AND ADDRESS THE PERKIN-ELMER CORPORATION NORWALK, CONNECTICUT 06856	16 10. PROGRAM ELEMENT, PROJECT, TASK AREA & WORK UNIT NUMBERS 62204F 2001 01 41 12/41	
11. CONTROLLING OFFICE NAME AND ADDRESS AIR FORCE AVIONICS LABORATORY AFAL/DHO WPAFB, OH 45433	11 12. REPORT DATE May 1977	13. NUMBER OF PAGES 63
14 14. MONITORING AGENCY NAME & ADDRESS (if different from Controlling Office) PF-12985 12/69	15. SECURITY CLASS. (of this report) UNCLASSIFIED	15a. DECLASSIFICATION/DOWNGRADING SCHEDULE
16. DISTRIBUTION STATEMENT (of this Report) DISTRIBUTION IS LIMITED TO U.S. GOVERNMENT AGENCIES ONLY BY REASON OF INCLUSION OF TEST AND EVALUATION OF DATA; APPLIED MARCH 1976. OTHER REQUESTS FOR THIS DOCUMENT MUST BE REFERRED TO AFAL/DHO WRIGHT-PATTERSON AIR FORCE BASE, OHIO 45433		
17. DISTRIBUTION STATEMENT (of the abstract entered in Block 20, if different from Report)		
18. SUPPLEMENTARY NOTES		
19. KEY WORDS (Continue on reverse side if necessary and identify by block number) CW LASER CONDUCTIVE YAG LASER COOLING PUMP LAMPS DEVICE ELECTRODELESS LAMPS		
20. ABSTRACT (Continue on reverse side if necessary and identify by block number) ✓ THE DEVELOPED ELECTRODELESS LAMP IS COMPATIBLE WITH CONDUCTIVE COOLING. IT HAS BEEN DEMONSTRATED THAT THE LIFE OF SUCH A LAMP HAS BEEN GREATER THAN 1000 HOURS OF OPERATION. FURTHERMORE, IT HAS BEEN DEMONSTRATED THAT AN OUTPUT OF ONE WATT MULTIMODE AT 1.06 MICRON CAN BE ACHIEVED FOR AN INPUT OF 215 WATTS OF RF POWER TO THE LAMP ↑		

DD FORM 1 JAN 73 1473 EDITION OF 1 NOV 65 IS OBSOLETE

UNCLASSIFIED

SECURITY CLASSIFICATION OF THIS PAGE (When Data Entered)

279 550

1B

FOREWORD

This technical report has been prepared by the Perkin-Elmer Corporation, Norwalk, Connecticut 06856, under Contract No. F33615-75-C-1193 for the Air Force Avionics Laboratory at Wright-Patterson Air Force Base, Ohio 45433.

The report covers the period of March 17, 1975 to March 18, 1976.

David A. Huchital was the principal scientist for the Perkin-Elmer Corporation. R.F. Paulson monitored this program for the Air Force (AFAL/DHO 55410).

ACCESSION for	
NTIS	White Section <input type="checkbox"/>
DDC	Buff Section <input checked="" type="checkbox"/>
UNANNOUNCED	<input type="checkbox"/>
JUSTIFICATION	
BY	
DISTRIBUTION/AVAILABILITY CODES	
Dis	SPECIAL
B	

## TABLE OF CONTENTS

SECTION		PAGE
I	INTRODUCTION	1
	1. High Power Nd:YAG: Results with Electrodeless Lamps	2
	2. Low Power Nd:YAG	2
II	ANALYSIS	7
	1. Analytical Model of a Nd:YAG Laser	7
	2. Thermal Analysis of a Lamp Module	13
	3. Diffuse Reflector Efficiency	16
	a) Rod Absorption	17
	b) Efficiency in a Simple Geometry	19
	c) Efficiency in a Complex Geometry	19
	4. Effect of Rod Quality	22
	5. Effect of Rod Diameter	22
III	MEASUREMENTS	24
	1. Coil Losses, $P_c$	24
	2. Lamp Threshold, $P_{Lo}$ and Lamp Radiation Efficiency, $\eta_1$	27
	3. Lamp Efficiency: Output in the Pump Bands	28
	4. Diffuse Reflector Efficiency	28
	5. Laser Rod Insertion Loss	34
IV	LASER PERFORMANCE	36
	1. Fabrication and Testing of SPL-1	36
	2. Fabrication and Testing of SPL-2	38
	3. Fabrication and Testing of SPL-3	44
V	LIFE TESTING	54
VI	CONCLUSIONS AND RECOMMENDATIONS	60

LIST OF ILLUSTRATIONS

FIGURE		PAGE
1	Conventional rf-YAG Laser	3
2	Results of 1000-Hour Life Test of rf-YAG Laser	4
3	Side-Pumped Laser (SPL) Configuration	6
4	SPL Lamp	9
5	Temperature Difference Between the Center and Edge of the Lamp Window vs. Power Input	15
6	Complex Diffuse Reflector Geometry	20
7	Calculated Slope Efficiency ( $\eta_s$ ) and Threshold Power ( $P_{th}$ ) for 3mm- and 4mm-Diameter Rods	23
8	Machining of SPL Coil	26
9	Plasma in SPL Lamp	29
10	Optimized Lamp Power Output	30
11	Rod Test Set-Up	35
12	The SPL-1	37
13	Diagram of SPL-1	39
14	Schematic of SPL-2	40
15	Performance of SPL-2	42
16	Performance of SPL-2a	43
17	Predicted Power Output as a Function of Rod Temperature	45
18	The SPL-3	46
19	Interior of SPL-3	47
20	Fixture for Testing the Efficiency of Heat Sink Adhesives	48
21	The SPL-3 in the Vicinity of the Rod	51
22	Anti-reflection Coating on Laser Rod from SPL-3	52
23	Life Test Arrangement	56
24	Precision Lamp Fabrication	58





## SECTION I

### INTRODUCTION

The Perkin-Elmer Corporation has, for several years, been pursuing a program in the pumping of Nd:YAG with electrodeless krypton arc lamps.<sup>(1-3)</sup> The approach leads to devices with improved efficiency, lifetime and reliability compared with conventional krypton lamp-pumped devices.

The research covered herein specifically addressed the applicability of the concept to a low-power, high-efficiency device suitable for operation in a space environment. Results show that a multimode output of 1 watt can be developed for approximately 200 watts of rf power. In addition, a 1000-hour lamp life test was successfully performed.

Section II of this report is an analysis of the efficiency and thermal considerations applicable to a low-power electrodeless lamp-pumped laser. Results show that the required output should be attainable for between 150 and 200 watts rf input and that conductive cooling of both lamp and laser rod is feasible.

Section III discusses a series of measurements aimed at quantifying the power flow within the laser. Each separate transfer or efficiency has been measured and is shown to agree with the assumptions and predictions made in Section II. The only exception was the insertion loss of the GFE (Government-furnished equipment) heat-sink-mounted laser rod which was shown to be anomalously high.

Section IV discusses the performance of the several lasers constructed during this program. The first, SPL-1 (for Side-Pumped-Laser-1) used the above mentioned GFE laser rod, while SPL-2 and SPL-3 used rods of different sizes.

Section V discusses the life testing program pursued on this contract. A 1000-hour life test was successfully completed on a conductively cooled lamp and a second test with a 5000-hour goal has begun.

Finally, Section VI presents our conclusions and recommendations for future work.

1. High Power Nd:YAG: Results with Electrodeless Lamps. The initial motivation for the electrodeless arc lamp approach was derived from the excruciating lifetime and reliability characteristics of dc-arc lamps. Most of the failure modes of arc lamps are associated with the electrodes and the fused silica-to-metal seals; consequently, electrodeless lamps should have notably greater utility. That radio-frequency energy can be used to drive an arc discharge was, of course, already well established. What was not clear, however, was whether the electrical energy could be efficiently coupled to the lamp and optical energy transmitted from the lamp to the rod with adequate efficiency to be competitive with dc-arc lamps. The task is a demanding one, as the requirements for efficient electrical and optical coupling are frequently disparate. The crucial element to the solution to the problem was the establishment of high efficiency optical coupling by means of a diffusely reflecting enclosure. Figure 1 illustrates the basic configuration of the device. The pump lamp is annular and surrounds the laser rod. Both are enclosed in a diffusely reflecting cylinder which is, in turn, surrounded by the rf coupling coil. This device developed 20 to 25 watts of multimode laser output from a 4x50mm laser rod for 1.5 kilowatts of rf energy input. Figure 2 illustrates the results of a 1000-hour life test. The power fall-off experienced in the course of the test was almost negligible. A final task on the above effort was the development of a high efficiency rf driver. A versatile, single-tube device was built based upon a 3CX1500A ceramic triode. The overall power supply efficiency, including the 208 VAC-HVDC conversion and the filament, relay, and blower power, was 63% in the master oscillator, power amplifier mode, and 67% in the self-excited oscillator mode.

The overall efficiency of the laser was slightly greater than 1% at an output level of 20 to 25 watts. The goal of this effort can be concisely stated as the development of a similarly long-lived device which develops one-tenth the output at the same power efficiency.

2. Low Power Nd:YAG. In the low-power region, the most highly developed

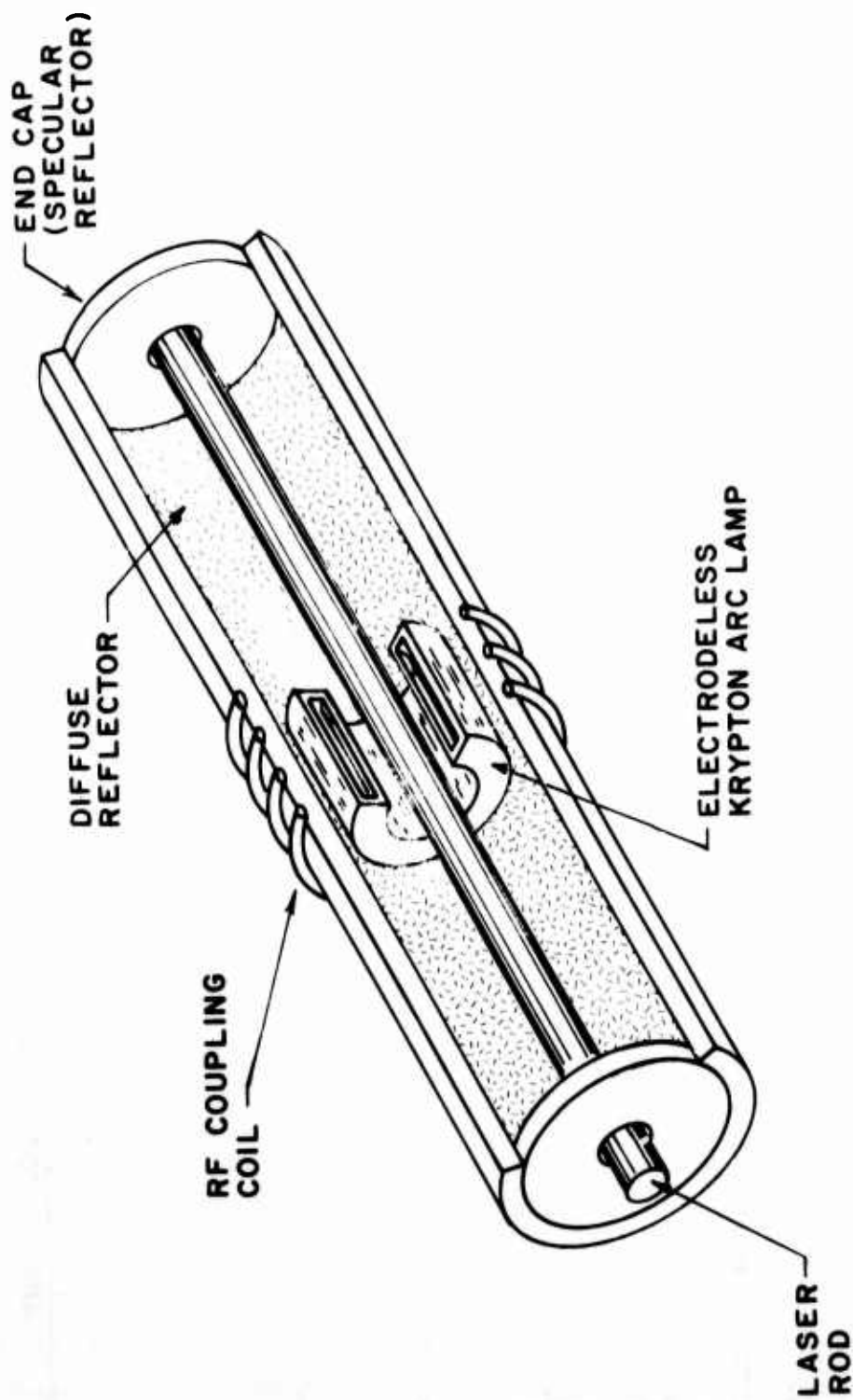


FIG. 1 CONVENTIONAL RF-YAG LASER

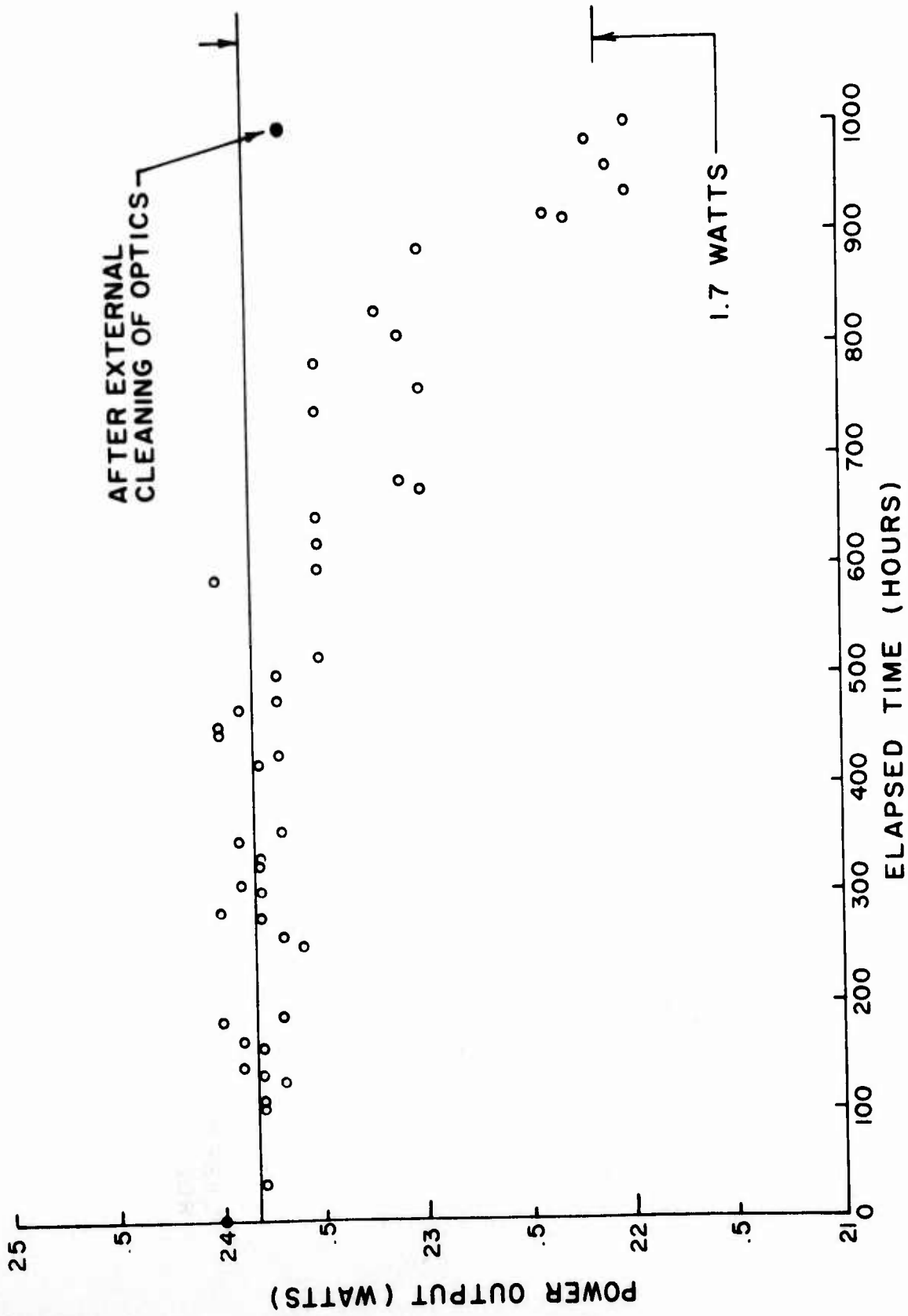


FIG. 2 RESULTS OF 1000 HOUR LIFE TEST OF RF-YAG LASER

pumping approach uses alkali-metal vapors in core-drilled sapphire envelopes. In this case, the most significant pathological phenomena appear to involve chemical reactions, erosion and decomposition of the envelope.

There is reason to believe that an electrodeless lamp approach could be developed which would obviate many of the failure modes observed in conventional alkali-metal lamps. However, our approach here has been to exploit the relatively straightforward technology associated with krypton-filled, fused silica envelopes.

The approach is still based upon an electrodeless krypton arc lamp and diffuse reflector. However, the requirement for conductive cooling of both lamp and laser rod required the development of an alternative structure to the coaxial scheme illustrated in Figure 1. The side-pumped laser illustrated in Figure 3 was proposed to satisfy these needs. The rod is cooled by conduction into a metal heat sink while the lamp is in thermal contact with the relatively cool diffuse reflector. A few watts are dissipated in the rod which must be maintained at a temperature of some  $-10^{\circ}\text{C}$ , while the lamp, which dissipates about 100 watts, can run at  $500^{\circ}\text{C}$  to  $600^{\circ}\text{C}$ .

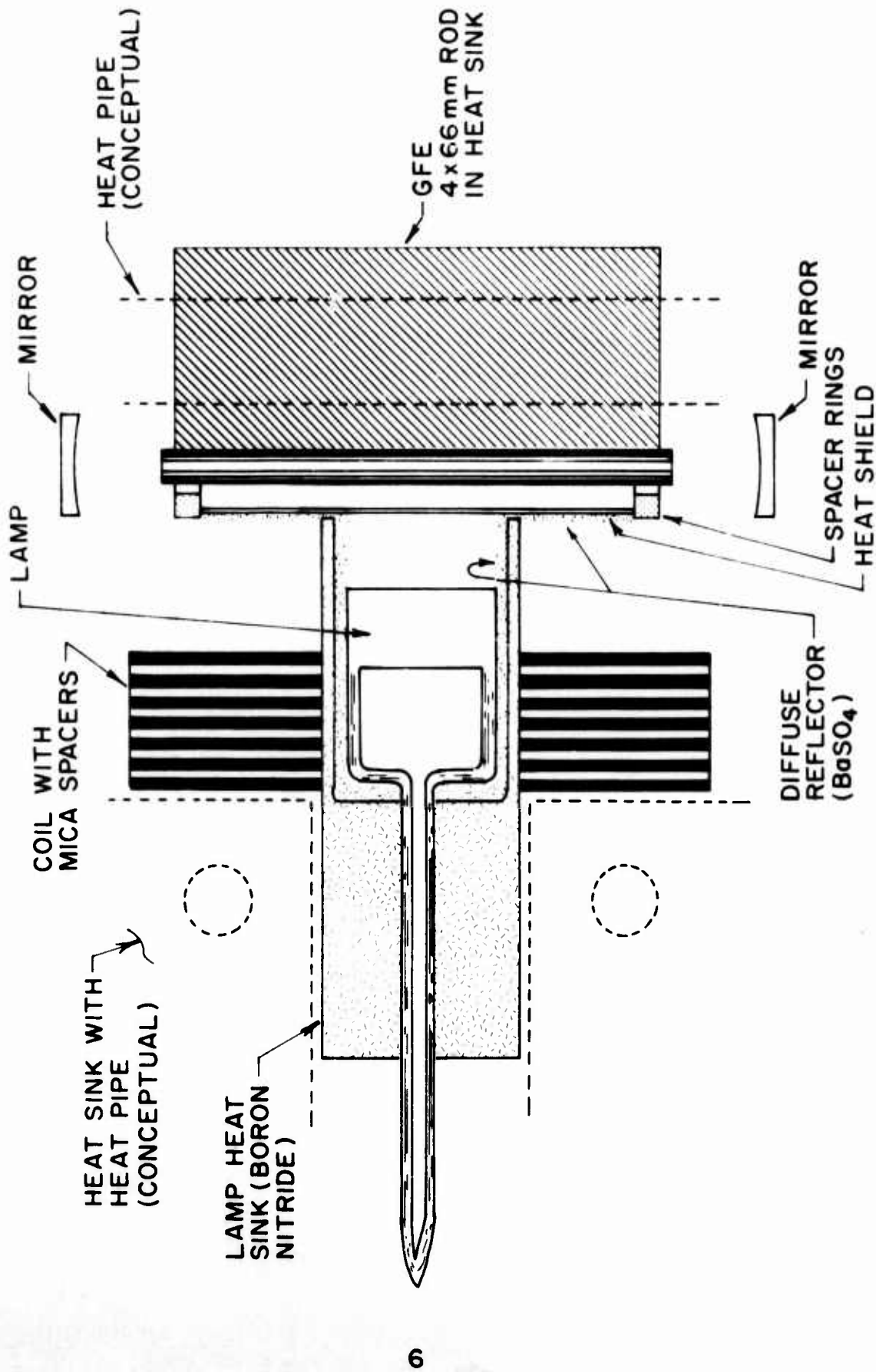


FIG. 3 SIDE PUMPED LASER (SPL) CONFIGURATION

## SECTION II

### ANALYSIS

This section considers the questions of laser efficiency, lamp cooling and lamp life from an analytical point of view. The issues are, of course, linked because greater efficiency implies less lamp power and consequent lower temperature and longer life.

#### 1. Analytical Model of a Nd:YAG Laser

We begin by defining the following quantities:

$P$  is the rf power delivered to the coil

$P_c$  is the power dissipated in the rf coupling coil

$P_{Lo}$  is the lamp threshold power

$\eta_1$  is the lamp slope efficiency

$P_L$  is the optical energy radiated by the lamp

The quantities  $P_c$ ,  $P_{Lo}$ ,  $\eta_1$  and  $P_L$  are related as follows:

$$P_L = \eta_1 (P - P_c - P_{Lo}) \quad (1)$$

Further, we define

$\eta_2$  is the fraction of the lamp energy which falls within the Nd:YAG pump band

$\eta_3$  is the optical transfer efficiency of the diffuse reflector

$\eta_4$  is the conversion efficiency from pump radiation to 1.06 $\mu$ m radiation

$\eta_{res}$  is the efficiency of the laser resonator

The power absorbed by the rod is

$$P_{rod} = \eta_2 \eta_3 P_L \quad (2)$$

A certain fraction of  $P_{rod}$ ,  $P_{rod|th}$  is used in reaching threshold. This is related to the power required from the lamp by

$$P_{L|th} = P_{rod|th} / (\eta_2 \eta_3)$$

which is, in turn, related to the rf power required by

$$P_{th} = \frac{P_{L|th}}{\eta_1} + P_{Lo} + P_c \quad (3)$$

The laser slope efficiency is

$$\eta_s = \eta_1 \eta_2 \eta_3 \eta_4 \eta_{res} \quad (4)$$

The goal of the subject RFP is the development of 0.5 watt  $TEM_{00}$  laser output. Our previous research indicates that a multimode-to-single-mode conversion efficiency,  $\eta_6$ , of 50% can be achieved even at higher power levels. Consequently, the total rf power required is

$$P = P_{th} + \frac{2}{\eta_s} P_{oo} \quad (5)$$

where  $P_{oo}$  is the desired  $TEM_{00}$  output power.

The lamp style of Figure 4 was developed as being compatible with the efficiency and cooling requirements of the program. The optimum parameters appear to be

fill pressure:	2 atm
D:	14 mm
t:	1 mm
$L_a$ :	9 mm
$L_w$ :	6 mm

The performance parameters of such a lamp were measured to be

$$P_c = 25 \text{ watts}$$



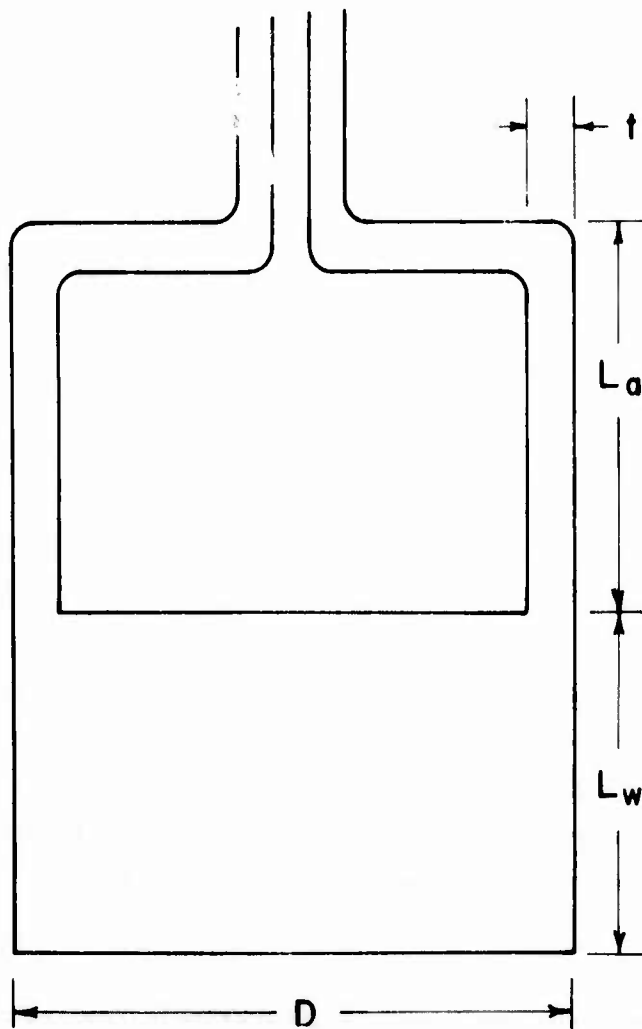


FIG. 4 SPL LAMP

$$P_{Lo} = 50 \text{ watts}$$
$$\eta_1 = 29\%$$

These measurements are discussed in Section III.

The parameter  $\eta_2$  was determined by measuring the fraction of the lamp output that was transmitted through a 10mm-thick, uncoated Nd:YAG filter. The same spectrally compensated silicon detector was used here as was used in determining  $\eta_1$  so that spectral effects were obviated. The resulting determination was  $\eta_2 = 0.39$ .

It is useful to compare these results with those obtained by Koechner.<sup>(4)</sup> He measured the product  $\eta_1 \eta_2$  to be 0.15 compared to our 0.11. The higher value achieved in his experiment is probably consistent with the high pumping level, but it is important to point out that our model is conservative compared with the prior art.

The efficiency of the diffuse reflector,  $\eta_3$ , has a design goal of 50%. The detailed design will be discussed in Section IV. This is identical to the values reported by Koechner<sup>(5)</sup> and inferred from the measurements of Foster and Osterink<sup>(6)</sup> for conventional optical coupling schemes.

References (5) and (6) do differ substantially on the question of the efficiency of the pumped rod. Koechner reported an overall efficiency of 2.1% while Foster and Osterink achieved 3.4%. However, most of the difference can be ascribed to the poor optical quality of Koechner's laser rod. The round-trip loss of 7.5% is much higher than generally observed for a good crystal, that is 0.2%/cm.

We can, however, use Foster and Osterink's results to estimate the rod quantum efficiency,  $\eta_4$ . Their measured slope efficiency,  $\eta_s$ , was 4%. Foster measured a heat generation rate of 190 watts for the rod when it was not lasing. However, it is reasonable to expect that some of the energy absorbed by the rod was radiated away as 1.06 $\mu$ m fluorescence. Shokin<sup>(7)</sup> has shown that the ratio of fluorescence cooling (in watts radiated) to laser power available is roughly 0.5. Now at 3kW input, Foster's rod developed 90 watts of laser output. Consequently, if we postulate that the

fluorescence cooling of Foster's rod was  $90/2 = 45$  watts, we arrive at a total absorbed energy of  $190 + 45$  or 235 watts. One third of this was used in reaching threshold, so that the efficiency of the rod-resonator combination above threshold is

$$\eta_4 \eta_{res} = \frac{90}{2/3 (235)} = 0.57$$

Further, if we postulate a round-trip-loss of 0.2%/cm and 0.1% scatter at every surface, we calculate  $\eta_{res}$ , for this example, to be 0.7. Thus,  $\eta_4$  is  $0.57/0.7$  or 0.8. In the calculations to follow, we will use a more conservative figure of 0.7 for  $\eta_4$ .

For our calculation of laser threshold, we use Kushida's value<sup>(8)</sup> for the small signal gain of Nd:YAG at 20°C.

$$g_{20} = 8.2 \text{ db/cm} - (\text{joule/cm}^3)$$

According to Ostermayer,<sup>(9)</sup> the gain at -10°C is 1.67 times greater than at room temperature owing to the reduced fluorescence linewidth.

Consequently,

$$g_{-10} = 13.7 \text{ db/cm} - (\text{joule/cm}^3)$$

For example, let us consider a 4x30mm laser rod. The round-trip gain is

$$g_{RT} = 218 \text{ db/joule}$$

Assuming a fluorescence lifetime of 230 $\mu$ s yields

$$g_r = 5 \times 10^{-2} \text{ db/watt}$$

If we further assume the scattering and absorption losses in the rod to be 0.2%/cm, that scatter at any surface amounts to 0.1% and that the

resonator includes a 1.5% output mirror, the net round-trip loss is 3.3%.  
Consequently, the power required to reach threshold is

$$P_{\text{rod}}|_{\text{th}} = 2.82 \text{ watts}$$

Further, if  $\eta_2 = .39$  and  $\eta_3 = .5$ , we can then calculate

$$P_L|_{\text{th}} = 14.5 \text{ watts}$$

And if  $\eta_1 = .29$ ,  $P_c = 25$  watts and  $P_{Lo} = 50$  watts, the rf power to the lamp is

$$P_{\text{th}} = 125 \text{ watts}$$

The laser slope efficiency is (based upon  $\eta_{\text{res}} = 1.5/3.3 = .45$ )

$$\eta_s = \eta_1 \eta_2 \eta_3 \eta_4 \eta_{\text{res}} = 1.8\%$$

So that the rf power required to develop one-half watt of  $\text{TEM}_{00}$  output is

$$P_{\text{rf}} = 181 \text{ watts (4mm rod, } \eta_3 = 0.5\%)$$

It is possible to predict the performance of other laser rod sizes based upon this model. For example, let us consider a 3x30mm laser rod. Assuming that we can achieve optical coupling efficiency,  $\eta_3$ , of 50%, we find

$$P_{\text{rod}}|_{\text{th}} = 1.59 \text{ watts}$$

$$P_L|_{\text{th}} = 8.15 \text{ watts}$$

$$P_{\text{th}} = 103 \text{ watts}$$

$$\left. \begin{array}{l} P_{\text{rod}}|_{\text{th}} = 1.59 \text{ watts} \\ P_L|_{\text{th}} = 8.15 \text{ watts} \\ P_{\text{th}} = 103 \text{ watts} \end{array} \right\} \begin{array}{l} 3\text{mm rod} \\ \eta_3 = 0.5 \end{array}$$

$$\eta_s = 1.8\%$$

$$P_{rf} = 159 \text{ watts}$$

Thus, the system based upon the 3x30mm rod will be more efficient than the 4x30mm based system by approximately 20 watts.

But if an optical coupling efficiency of 50% is the best we can achieve with a 4mm rod, it is reasonable to believe that  $\eta_3$  will be less than 0.5 for a 3mm rod. Indeed, in Section V we show that it should be 0.31. In this case

$P_{rod th}$	= 1.59 watts	}	3mm rod $\eta_3 = 0.31$
$P_L th$	= 13.2 watts		
$P_{th}$	= 120 watts		
$\eta_s$	= 1.1%		
$P_{rf}$	= 210 watts		

Clearly, under these conditions, the 4x30mm system is preferable.

## 2. Thermal Analysis of the Lamp Module

In this section, we consider the thermal analysis of the lamp and diffuse reflector configured as shown in Figure 4. Here

- t is the wall thickness of the lamp
- D is the lamp diameter (outside)
- $(L_a - t)$  is the length of the active part of the lamp
- $L_w$  is the window thickness
- $t_1$  is the gap between the lamp and the diffuse reflector
- $t_2$  is the thickness of the diffuse reflector

The hottest point on the lamp will be the center of the inside surface of the window. The temperature profile of this surface can be shown to be

$$T(r) = \frac{W}{4kL_w} \left[ \left( \frac{D}{2} \right)^2 - r^2 \right] \quad (6)$$

where  $W$  is the thermal load on the window and  $k$  is its thermal conductivity. We assume that of the power input to the lamp, 29% is radiated away to be dissipated elsewhere. Further, we take

$$D = 14\text{mm}$$

$$L_w = 6\text{mm}$$

$$k = 0.017 \text{ w/cm-}^\circ\text{K}$$

Figure 5 is a plot of the temperature in the center of the window as a function of the total rf power for various values of the window thickness,  $L_w$ . The parameter  $\Delta T$  of Figure 5 designates the temperature difference between the window center and the interface between lamp and reflector.

The present design calls for a gap between the lamp and the diffuse reflector of less than 0.004mm. However, during operation, differential thermal expansion can increase the gap by an order of magnitude. Consequently, if we take the thermal drop conductivity of air to be  $4.5 \times 10^{-4} \text{ w/cm-}^\circ\text{K}$ , we find a temperature drop across the gap of 1.1 degrees per watt of lamp dissipation. Thus, for a total rf input lamp of 180 watts, the temperature difference across the gap will be  $121^\circ\text{C}$ . If we assume that the outside of the diffuse reflector operates at  $100^\circ\text{C}$ , reference to Figure 5 reveals that with a 6mm thick window the maximum temperature will appear in the center of the lamp window and will be of the order of  $500^\circ\text{C}$ . Lamp life at this temperature should be very long.

The final questions involve thermal stress on the lamp and diffuse reflector. We have previously shown that lamps of similar geometry are within the thermal stress limits at rf power levels of 1.0 to 1.5 kW.

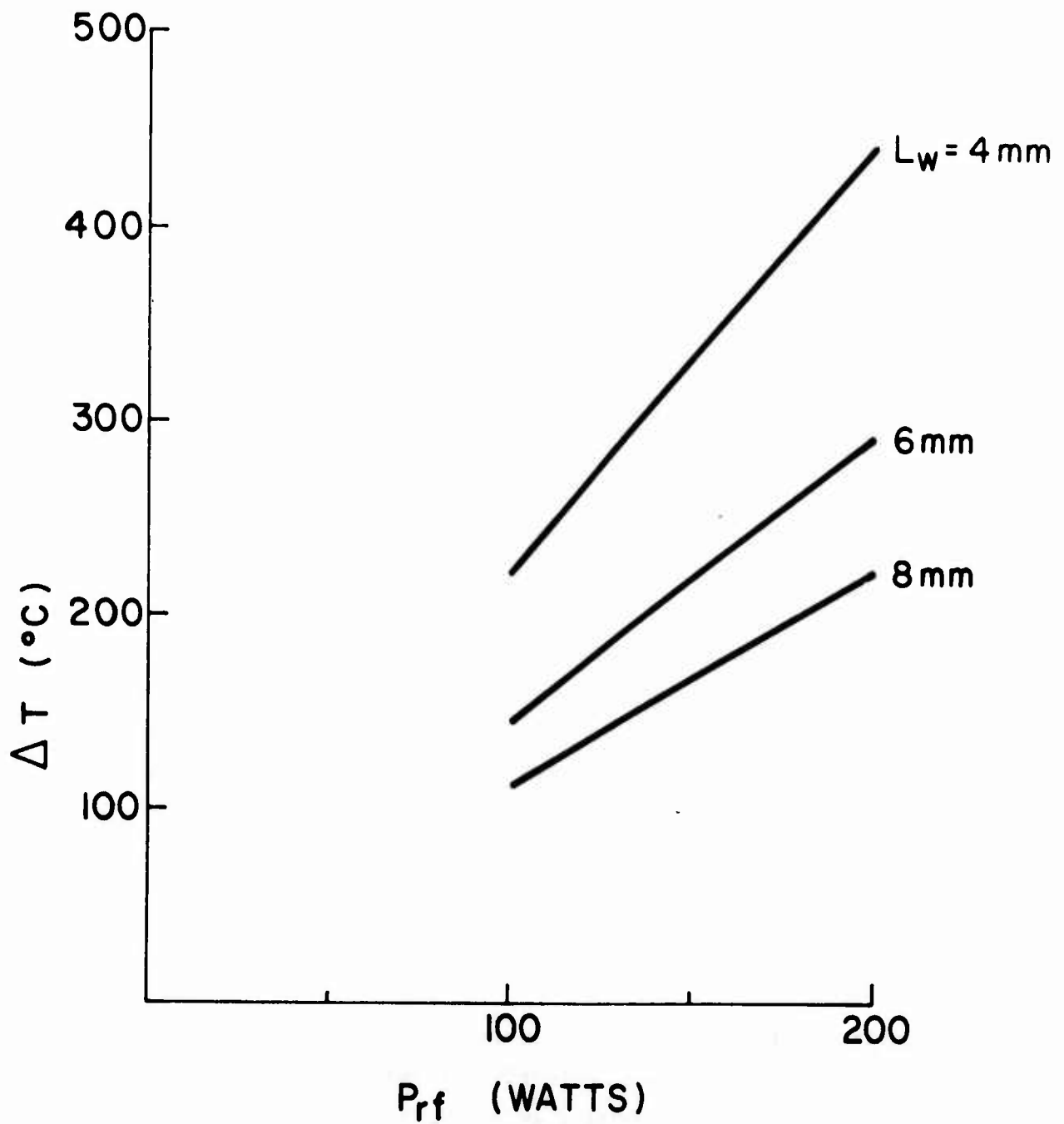


FIG. 5 TEMPERATURE DIFFERENCE BETWEEN THE CENTER AND EDGE OF THE LAMP WINDOW vs. POWER INPUT

In the case of the diffuse reflector, Thouret<sup>(10)</sup> shows that a uniformly loaded cylinder of the inner radius  $r_1$  and outer radius  $r_o$  is under an azimuthal stress of

$$\sigma_{\theta} = W \frac{c}{2} \left[ r_1 + r_1 \ln \frac{r_o}{r_1} - \frac{r_o^2 r_1}{r_o^2 - r_1^2} \left( \frac{r_1^2}{r_o^2} + 1 \right) \ln \frac{r_o}{r_1} \right] \quad (7)$$

where

$$c = \frac{\alpha E}{k(1-\mu)}$$

$\alpha$  is the thermal expansion coefficient

$\mu$  is the Poisson ratio

$W$  is the thermal loading per unit area

$E$  is the modulus of elasticity

which, for alumina at 100°C yields a result of 5 psi per watt of input energy. Since the ultimate tensile strength of alumina is approximately  $2.5 \times 10^4$  psi, the structure should be well within safe limits. We should point out, parenthetically, that at high power levels it becomes important to cool the alumina adequately as its thermal conductivity, and thus the thermal stress, are strong functions of temperature. At 600°C, the thermal stress works out to 28 psi/watt.

### 3. Diffuse Reflector Efficiency

The earliest diffuse reflector geometries were cylindrical with the rod located on axis. We assume that scattering at the surface of the diffuse reflector was isotropic and developed an expression for the optical coupling efficiency. Subsequently, we discovered a paper by Whittle and Skinner<sup>(11)</sup> who presented the results of a Monte-Carlo analysis of the problem and compared it with experimental data. They also considered a very simple model, based again upon an isotropic assumption. In the simple model a surface of area  $S_1$  absorbs a fraction

$$F_1 = S_1 / \Sigma S_1 \quad (8)$$



of the total. The formula can easily include the effects of finite absorptivity,  $B_i$ ,

$$F_i = S_i B_i / \sum S_i B_i \quad (9)$$

Whittle showed that the predictions of the simple model agreed well with those of the more sophisticated Monte-Carlo model.

For example, if a reflector has a total surface area of  $S_r$  with a reflectivity  $\rho$ , the effective loss area is  $(1-\rho) S_r$ . If the reflector includes a hole that totals  $S_h$ , and if the load, the laser rod can be approximated by a hole of size  $S_L$ , the efficiency of the structure will be

$$\eta = \frac{S_L}{S_L + S_h + (1-\rho) S_r} \quad (10)$$

Two additional calculations are required to relate this simple model to an actual SPL.

- The absorbing power of the laser rod must be calculated, and
- The model must be corrected for the non-uniform illumination levels which occur in some versions of the SPL. In particular, models SPL-1, 2 and 2a had a large chamber pumping the center of the rod and two smaller chambers occupying the end sections.

a. Rod Absorption - We have previously measured and reported<sup>(12)</sup> the absorption constants for each of the prominent krypton emission lines. The result is reproduced in Table I along with the relative strength of the various lines.

The task of computing the average path length through the rod is greatly simplified by the high index of YAG. The effect is to bend all rays strongly toward the axis of the rod, so that the path length approaches the rod diameter. A ray incident at an angle of  $70^\circ$  from a radius but perpendicular to the axis will pass through the rod at an angle of  $31^\circ$ , and its path length will be 0.86 times the rod diameter. Similarly, rays incident

TABLE I  
 ABSORBANCE OF KRYPTON LINES IN Nd:YAG

Wavelength (Å)	Absorbance (mm <sup>-1</sup> )	Relative Strength
7587	0.045	0.33
7601	0.083	1.00
7685	0.012	Weak
7694	0.007	Weak
7854	0.016	Weak
8059	0.146	0.18
8104	0.059	0.28
8112	0.074	0.75
8190	0.023	0.13
8263	0.006	Weak
8281	0.002	Weak
8298	0.008	Weak

at an angle to the rod axis will be refracted toward it. The path length for the more oblique of these rays may be slightly greater than the rod diameter; however, this effect will be very nearly balanced since a fraction of these rays will be reflected at the air-rod interface.

For example, a ray incident at  $45^\circ$  to the rod axis will propagate through the rod at  $67^\circ$ . Its path length in the rod will thus be 1.09 rod diameters. However, 9.5% of the rays thus incident will be reflected so the fractional absorption will be very comparable to that for normally incident radiation.

Thus, if we take the average path as the rod diameter and choose  $0.08\text{mm}^{-1}$  as an average absorptivity for a strong line, we find that for a 3mm-diameter rod the absorbing power is 42% and for a 4mm-diameter rod it is 52%, that is

$$3\text{mm rod absorbing power} = 1 - 10^{(-3\text{mm} \times .08\text{mm}^{-1})}$$

$$4\text{mm rod absorbing power} = 1 - 10^{(-4\text{mm} \times .08\text{mm}^{-1})}$$

b. Efficiency in a Simple Geometry. Let us consider first a simple geometry where the 4mm-laser rod is located on the axis of a diffusely reflective cylinder of diameter D, length L and reflectivity  $\rho$ .

The cross-sectional area of the "hole" represented by the rod is  $4L \text{ mm}^2$  which, when loaded by the appropriate absorptivity, becomes  $2.1L \text{ mm}^2$ . The efficiency of the structure is thus

$$\eta_3 = \frac{2.1L}{2.1L + \left[ \pi DL + 2\pi \left( \frac{D}{2} \right)^2 \right] (1-\rho) + S_h} \quad (11)$$

where  $S_h$  is the area of any holes or cracks in the structure and all dimensions are in mm.

c. Efficiency in a Complex Geometry - Let us consider the geometry of SPL-1 and SPL-2. The appropriate dimensions are shown in Figure 6.

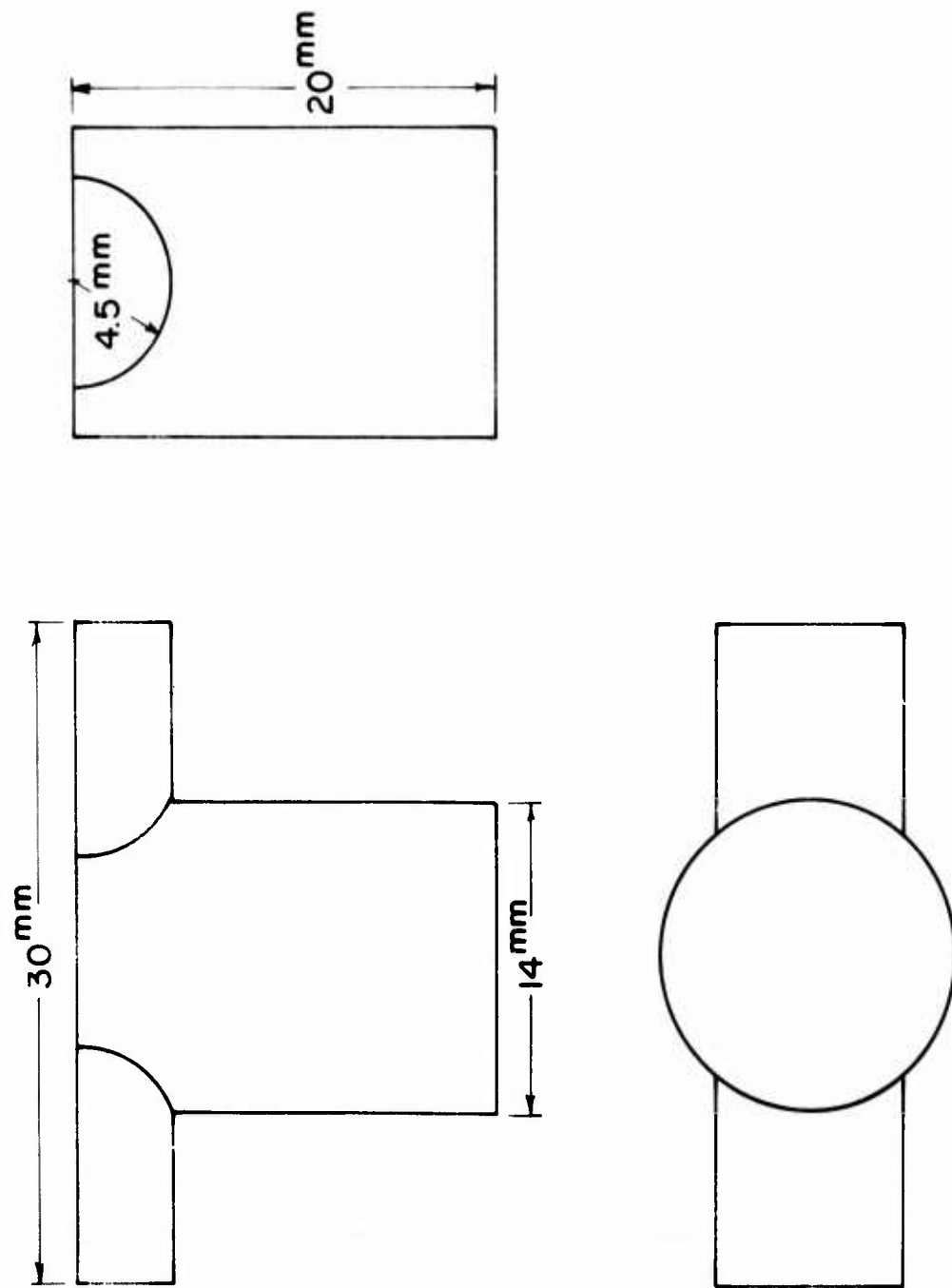


FIG. 6 COMPLEX DIFFUSE REFLECTOR GEOMETRY

Clearly, the problem is complicated by the fact that the light flux is non-uniform. Some of the light emitted by the lamp passes into the smaller chambers, but much of it is reflected back to the main chamber.

We can develop a solution in terms of loss coefficients,  $C_1^j$ . The superscript  $j$  refers to the chamber being considered. The main chamber will be "1" and the two smaller chambers will both be denoted "2". The subscript  $r$  will refer to power absorbed by the rod, "1" to power lost either by absorption in the diffuse reflector or by leakage out of the chamber, and "h" to energy transmitted into an adjoining chamber. Thus, the coefficient for absorption by the rod in the main chamber is denoted  $C_r^1$ .

The fraction of the energy that passes from the main chamber to the adjacent chamber is

$$F_h^1 = \frac{C_h^1}{C_r^1 + C_1^1 + C_h^1} \quad (12)$$

Of this energy, a part,  $F_h^2$  is reflected back.

$$F_h^2 = \frac{C_h^2}{C_r^2 + C_1^2 + C_h^2} \quad (13)$$

Thus, we can define an effective coupling fraction as

$$F_{h|eff}^1 = F_h^1 (1 - F_h^2) \quad (14)$$

$$F_{h|eff}^2 = F_h^2 (1 - F_h^1) \quad (15)$$

Similarly, we can define effective loss coefficients as

$$F_{h|eff}^1 = C_{h|eff}^1 / (C_{h|eff}^1 + C_r^1 + C_1^1) \quad (16)$$

$$F_{h|eff}^2 = C_{h|eff}^2 / (C_{h|eff}^2 + C_r^2 + C_1^2) \quad (17)$$

The chambers are now mathematically uncoupled. In the big chamber, the fraction of the energy absorbed by the rod is

$$F_r^1 = \frac{C_r^1}{C_r^1 + C_l^1 + C_{h|eff}^1} \quad (18)$$

and in the little chamber

$$F_r^2 = \frac{C_r^2}{C_r^2 + C_l^2 + C_{h|eff}^2} \quad (19)$$

The overall efficiency is

$$\eta_3 = F_r^1 + 2F_{h|eff}^1 \times F_r^2 \quad (20)$$

#### 4. Effect of Rod Quality

In the analysis above, we have assumed the availability of a laser rod with a combined scattering-absorption loss of  $2 \times 10^{-3} \text{ cm}^{-1}$ . Reference to the literature in the field<sup>(13)</sup> indicates this to be a reasonable assumption as do measurements reported in Section III. Nevertheless, it is appropriate to explore the implications of higher and lower loss values on the performance predicted by our model. Figure 7 is a summary of the predictions of the model for both 3 and 4mm rods as functions of the round trip loss.

#### 5. Effect of Rod Diameter

It is useful to calculate the change in diffuse reflector efficiency incurred if the rod diameter alone is allowed to vary. In a simple geometry, that is, one where the light flux is uniform, we can calculate  $\eta_3$  in terms of the rod absorption per bounce  $C_r$  and the losses per bounce  $C_l$  as  $\eta_3 = C_r / (C_r + C_l)$ . The rod absorption for a 4mm rod is stronger than that for a 3mm one by virtue of the larger aperture it presents (4/3) and by the greater path length for an incident photon. This latter factor is calculated to be (.52/.42) in Section II.3.a. Consequently,  $C_r$  is reduced by a factor of 0.61 for a 3mm rod compared to a 4mm one. For the example of a 4mm rod in a diffuse reflector achieving  $\eta_3 = 0.5$ , we can predict that  $\eta_3$  will be 0.31 for a 3mm diameter rod.

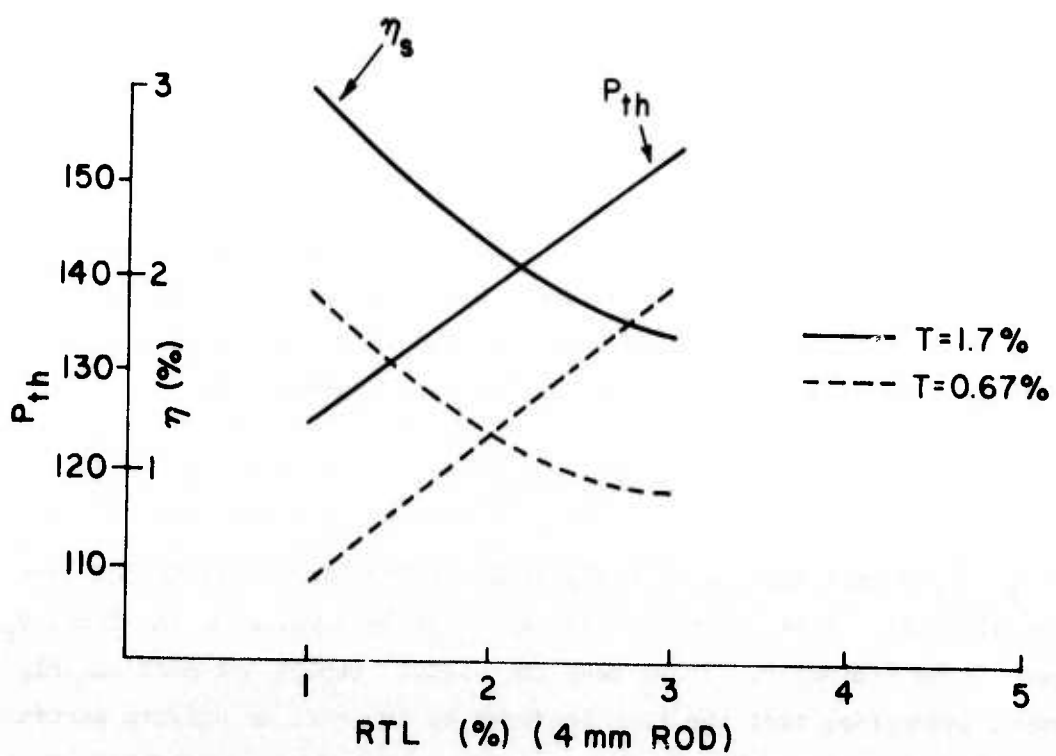
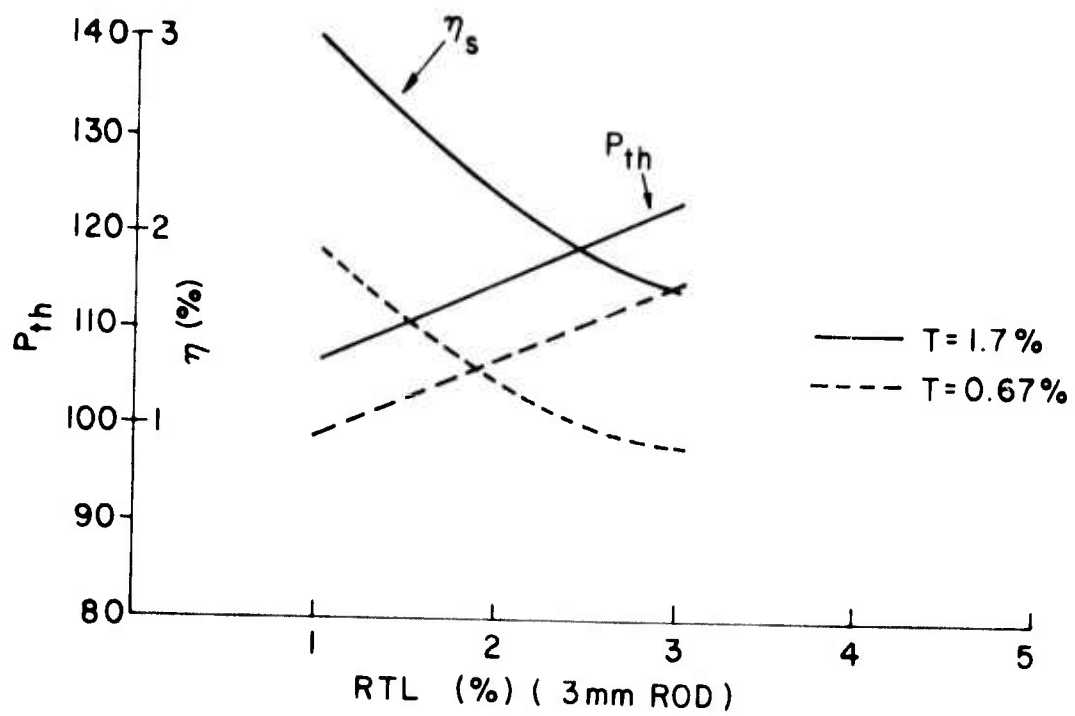


FIG. 7 CALCULATED SLOPE EFFICIENCY ( $\eta_s$ ) AND THRESHOLD POWER ( $P_{th}$ ) FOR 3mm AND 4mm DIAMETER RODS

### SECTION III

#### MEASUREMENTS

The difficulty experienced in generating comprehensive laser data led to increased emphasis upon measurements relating to the various components of the laser head. This section discusses observations of

- $P_c$ , the power dissipated in the rf coupling coil
- $P_{Lo}$ , the lamp threshold power
- $\eta_1$ , the lamp slope efficiency
- $P_L$ , the optical energy radiated by the lamp
- $\eta_2$ , the fraction of the lamp energy which falls within the Nd:YAG pump band, and
- $\eta_3$ , the optical transfer efficiency of the diffuse reflector

#### 1. Coil Losses, $P_c$

The voltage gradient necessary to drive a high-pressure krypton arc  $E_p$  is generally of the order of 20 V/cm. The total voltage required is thus

$$V_p = E_p l \quad (1)$$

where  $l$  is the plasma length. In the case of the lamp shown in Figure 1,  $l$  is the mean circumference of the lamp. When the lamps are excited by a coupling coil of  $n$  turns with inductance  $L_c$  and cross-sectional area  $A_c$ , the voltage induced in the coil when driven at frequency  $\omega$  is

$$V_c = \omega L_c I_c - V_b$$

where  $V_b$  is the back EMF due to the plasma current, and  $I_c$  is the current through the coil. Unless the coil is very closely coupled to the lamp,  $V_b$  can usually be neglected. If we make the useful, though not particularly rigorous, assumption that the flux produced by the coil is uniform across it, then

$$V_p = (1/n)(A_p/A_c)V_c = (1/n)kV_c \quad (2)$$



where  $A_p$  is the area linked by the plasma. Finally, the power dissipated in the coil is

$$P_c = \frac{V_c^2}{\omega L_c Q} = \frac{n^2 V_p^2}{\omega L_c Q k^2} \quad (3)$$

where the Q of the coil is defined in terms of its resistance, R, by

$$Q = \frac{\omega L_c}{R}$$

The quantities  $L_c$  and Q can be readily determined by the Q meter measurements and the voltage across the coil is easily measured with an rf voltmeter. Typically, we observe  $L_c = 0.5$  to  $1.0 \mu\text{H}$ ,  $Q = 250$  to  $400$  and  $V_c$  between  $800$  and  $1000$  volts leading us to predict that  $P_c$  will fall between  $15$  and  $25$  watts.

Low loss coils are fabricated by machining solid OFHC copper bars as shown in Figure 8. In the case where the lamp outer diameter is  $14\text{mm}$  we have found that a coil with

number of turns, n	= 5
inner diameter	= 18mm
outer diameter	= 35mm

exhibits an inductance of  $0.7 \mu\text{H}$  and a Q of  $330$ .

When used to drive an optimized lamp, the coil voltage is nearly  $1000$  volts, leading to a calculated coil loss of  $25$  watts. This parameter can be measured directly by observing the power required to develop  $1000$  volts across the coil with the lamp extinguished. The result is  $28$  watts.

It is reasonable to consider whether appropriate design could reduce  $P_c$  still further. Increasing the number of turns increases both  $L_c$  and Q, but equation (3) indicates that the overall effect on coil losses will be small. Another approach would be to make a coil that fits the lamp very closely. It might be possible to polish the inner surface of the coil so that it could

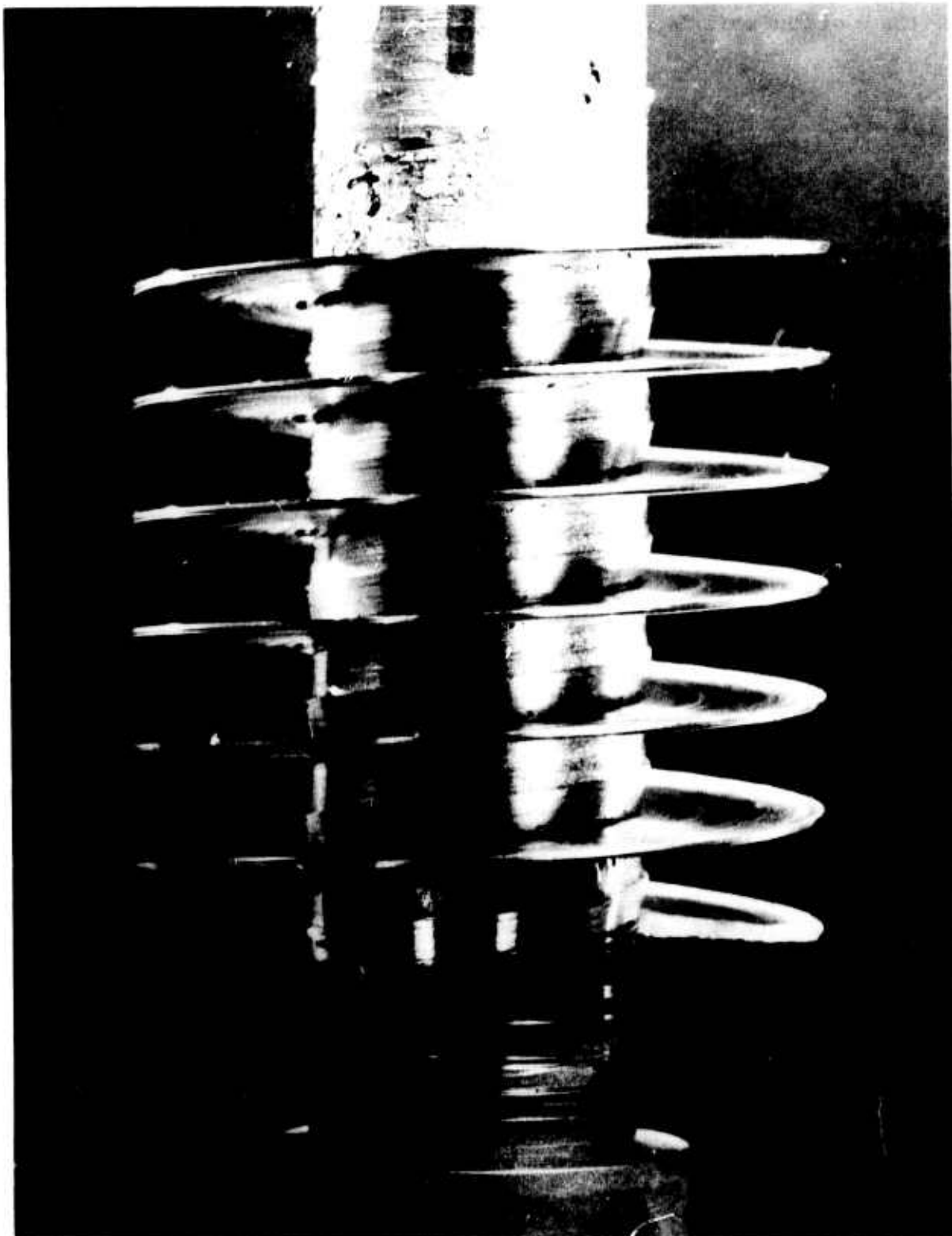


Figure 8. Machining of SPL Coil

fulfill the role presently played by the diffuse reflector. Coil loss measurements indicate that the tighter electrical coupling thus achieved drops the required voltage by about 30%, resulting in a coil loss of 12 watts. However, the approach is sufficiently difficult to implement that we have deferred further consideration.

## 2. Lamp Threshold, $P_{L0}$ and Lamp Radiation Efficiency, $\eta_1$

Lamp output was measured with an International Light Power Meter which incorporated a filter designed so that the spectral response of the filter-detector combination was spectrally flat. The detector was  $1 \text{ cm}^2$  and was usually positioned about 50cm from the freely radiating lamp. The optical flux was generally of the order of  $1 \text{ mw/cm}^2$  and thus the detector operated well within its linear range. In addition, the detector was checked against a calibrated Epply thermopile at 6328A and agreement was within 10%.

The radiating plasma approximated a cylinder 14mm in diameter and 8mm long and thus appeared as an extended source at a distance of 50cm. The radiation pattern was mapped and the radiated flux was found to approximate

$$p(\theta) = I(0.67 + 0.33 \cos \theta)$$

where  $\theta$  is the angle between the plasma axis and the detector.

For example, the on-axis radiated flux,  $I = p(0)$  from optimized lamps was  $9.5 \times 10^{-4} \text{ w/cm}^2$  at 150 watts input to the coil leading us to calculate a total lamp flux,  $\int_{-\pi/2}^{\pi/2} p(\theta) d\theta$  of about 22 watts.

The cold fill pressure was one of the more important parameters we investigated. Previous optimization exercises<sup>(14)</sup> had indicated that overall rf-YAG laser efficiency showed a broad maximum in the pressure range from 2.0 to 3.5 atmospheres. In the case of the SPL geometry we observed an additional effect. At fill pressures above about 2.5 atmospheres, the plasma showed a distinct tendency to float and to form a tight ball at the top of the lamp. This effect had two deleterious results. First the plasma would tend to overheat the envelope locally, and second, the small plasma

was inefficiently coupled to the rf field, resulting in high coil losses. (It is arguable that the effect would vanish in a gravity-free environment.) Consequently, we settled upon two atmospheres as being an optimum fill. As shown in Figure 9, page 29, the plasma still has a tendency to float at low power levels, but it is nearly symmetric in the region of interest.

Performance of an optimized lamp is summarized in Figure 10. The lamp was configured as shown in Figure 4 with  $t = 1\text{mm}$ ,  $L_a = 9\text{mm}$ ,  $D = 14\text{mm}$ ,  $L_w = 6\text{mm}$  and a fill of two atmospheres of krypton. The system shows a threshold of 75 watts. If we subtract the coil losses of 25 watts, we arrive at a lamp threshold  $P_{Lo}$  of 50 watts. Finally, we can extract the lamp slope efficiency,  $\eta_1$ , of 0.29.

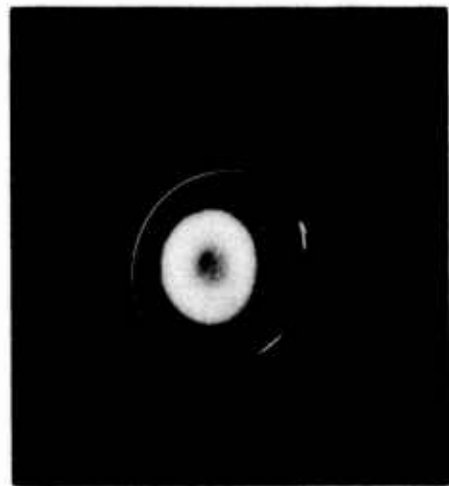
### 3. Lamp Efficiency: Output in the Pump Bands

The fraction of the lamp output falling in the Nd:YAG pump band was measured by observing the fraction of the lamp radiation that passed through a 1cm thick 1% Nd in YAG filter. Radiation flux was measured using the same detector as identified in subsection 2 above. Thus, any errors due to non-constant spectral response were obviated. The filter was uncoated so that its reflection coefficient for normally incident radiation should have been 8.6% per surface, which is in good agreement with a measurement made at 6328Å. When the data are corrected for reflection, we calculate that 39% of the lamp radiation is absorbed in the filter. Now, the filter was only thick enough to absorb about 90% of the in-band radiation; however, we have so far neglected the effects of scatter and out-of-band absorption in the crystal. Consequently, we will use the 39% figure in all subsequent calculations, that is,  $\eta_2 = 0.39$ .

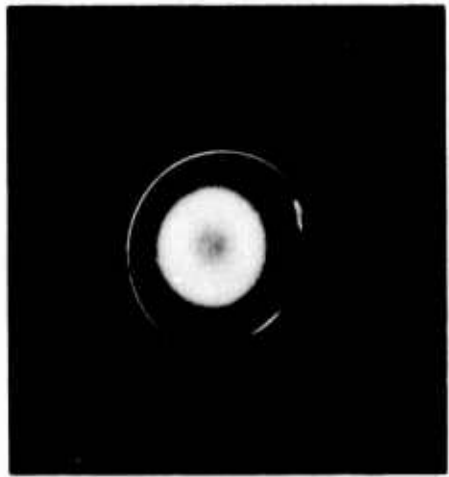
### 4. Diffuse Reflector Efficiency

The diffuse reflector efficiency was measured directly in SPL-2. The light in both the large and small chambers was measured with a 4x50mm laser rod in place and repeated with the laser rod replaced by a glass one. The ratios of the strengths of the various pump lines are summarized in Table II.

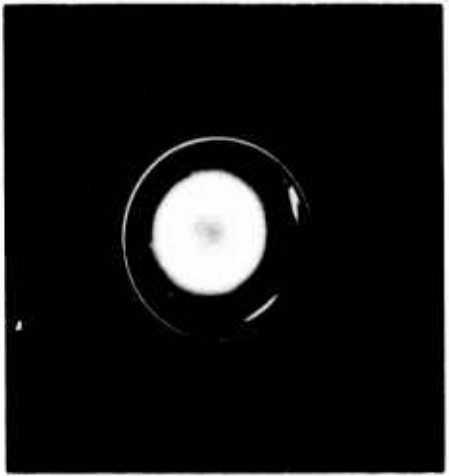
The necessity to disturb the optical circuit to change rods probably led to some errors in the data. In addition, some slight drift in the rf power



110 WATT



135 WATT



150 WATT

PLASMA IN SPL LAMP

FIG. 9

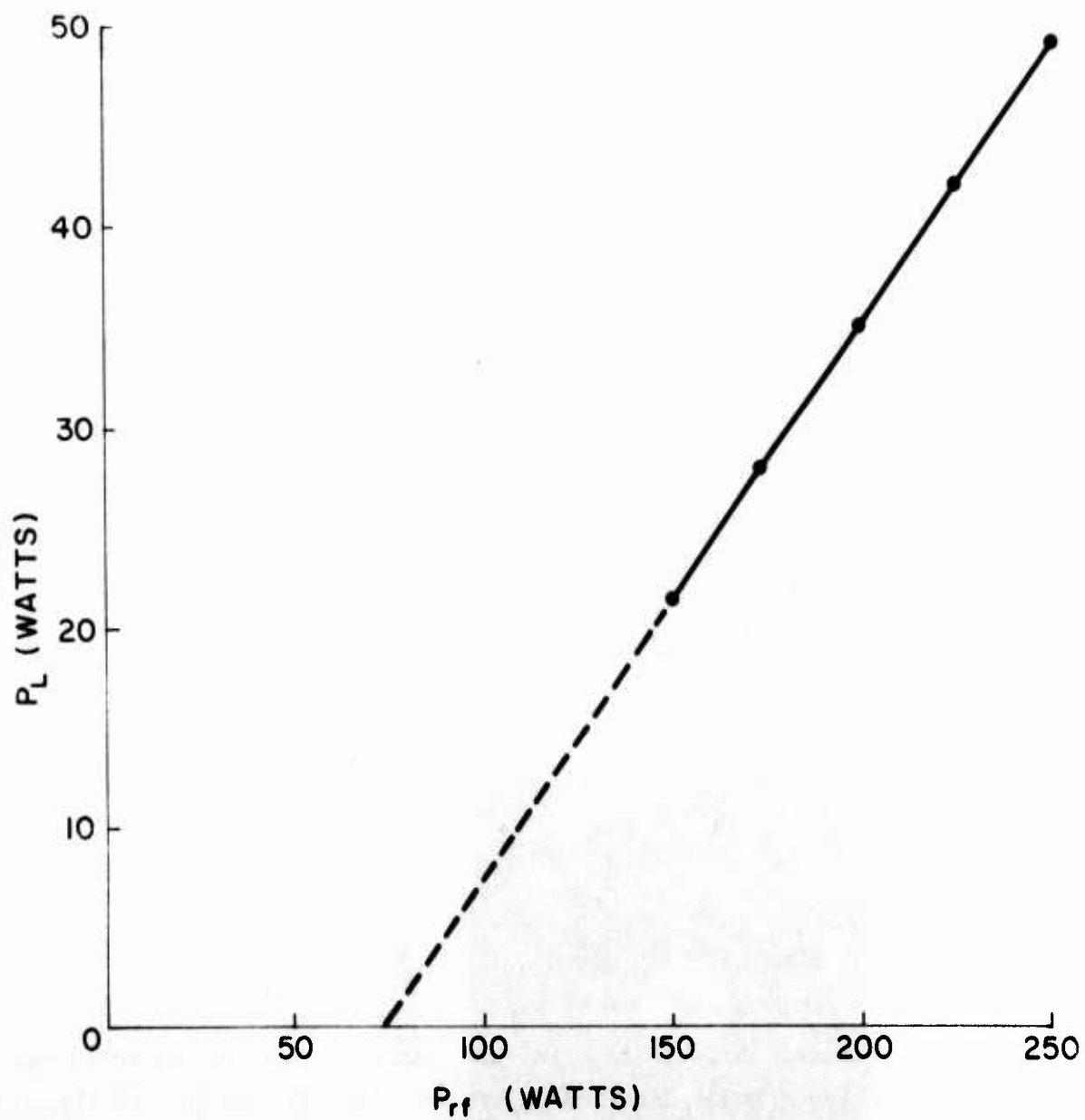


FIG. 10 OPTIMIZED LAMP POWER OUTPUT

level was unavoidable, and because of the nature of the measurement, it could lead to further errors. However, let us take 0.2 as the average value of the line absorption efficiency in chamber 1 and 0.6 for chamber 2. It is instructive to compare these results with the analysis of Section II. To be sure, the theoretical prediction is determined, to a large extent, by the estimates of the losses at each reflection from the diffuse reflector; however, for the sake of illustration, let us choose a nominal figure of 2% per reflection. We then calculate

$$F_h^1 = 0.665 \qquad F_h^2 = 0.56$$

and if we assume losses of 2% per reflection in both chambers

$$\begin{aligned} F_h^1|_{\text{eff}} &= 0.29 & F_h^2|_{\text{eff}} &= 0.19 \\ C_h^1|_{\text{eff}} &= 1.5\% & C_h^2|_{\text{eff}} &= 1.67\% \end{aligned}$$

From these results, we can calculate the theoretical absorption efficiency in chamber 1

$$F_r^1 = 0.26$$

and in chamber 2

$$F_r^2 = 0.59$$

and a net efficiency

$$\eta_3 = 0.63$$

The results for  $F_r^1$  and  $F_r^2$  are in acceptable agreement with the measurements summarized in Table II. We conclude that the diffuse reflector efficiency  $\eta_3$  for laser model SPL-2 was close to 0.5. The result for the fractional absorption efficiency in chamber 1 is somewhat higher than the measured value while the results in chamber 2 are in good agreement. One

TABLE II  
 ABSORPTION IN VARIOUS LINES IN SPL-2

Wavelength	$\alpha(\text{mm}^{-1})$	Rel. Line Strength	Fractional Absorption Efficiency	
			Chamber 1	Chamber 2
7601 <sup>o</sup> A	0.083	1.00	0.13	0.69
8112	0.074	.75	0.21	0.63
7587	0.045	.33	0.19	0.58
8104	0.059	.28	0.20	0.57
8059	0.146	.18	0.17	0.81
8190	0.023	.13	0.22	0.4



TABLE III

## ROD QUALITY

Rod No.	Description	$\Delta P_{th}$	Round-Trip-Loss
1	GFE 4x66mm	200 watts	6.7%
2	GFE 3x30mm	170 "	5.7%
3	P-E 4x50mm	100 "	3.3%
4	P-E 3x25mm	70 "	2.3%
5	P-E 3x50mm	170 "	5.7%
6	P-E 6x25mm	50 "	1.7%
7	P-E 4x50mm	110 "	3.7%
8	P-E 5x50mm	190 "	6.3%

can thus infer that the 2%-per-reflection figure is probably too low in chamber 1. However, the more significant conclusion is that both the analytical and experimental analyses support the assumption of an optical coupling efficiency of approximately 50%.

#### 5. Laser Rod Insertion Loss

The question of the laser rod round-trip-loss (RTL) is of paramount importance as it affects both the power required to reach threshold as well as resonator efficiency,  $\eta_{res}$ .

Laser rods were evaluated by inserting them in a cavity with a second, pumped rod and measuring the incremental power input to the second rod necessary to reach threshold,  $P_{th}$ . The test rod was carefully aligned to minimize  $P_{th}$ . The experiment is illustrated in Figure 11.

The quantity  $P_{th}$  can be related to RTL by an analysis similar to that of Section II. We assume the pumped rod reached 20°C when it was pumped, and take the 20°C gain as 8.2 db/cm - (joule/cm<sup>3</sup>). Further, we assume that the pumping efficiencies of the pumped rod were  $\eta_1 = 0.4$  and  $\eta_3 = 0.3$ . The lower diffuse coupling efficiency has been measured directly<sup>(15)</sup> and is consistent with the looser optical coupling of the racetrack rf-YAG configuration. From this point, we can relate the power input of the lamp of the pumped rod to its gain and to the loss introduced by the test rod.

The results of the measurements and calculations are summarized in Table III. The best rods have losses near 0.2%/cm as we assumed in Section II, but some, in particular the GFE 4x66mm rod, exhibited substantially higher losses.

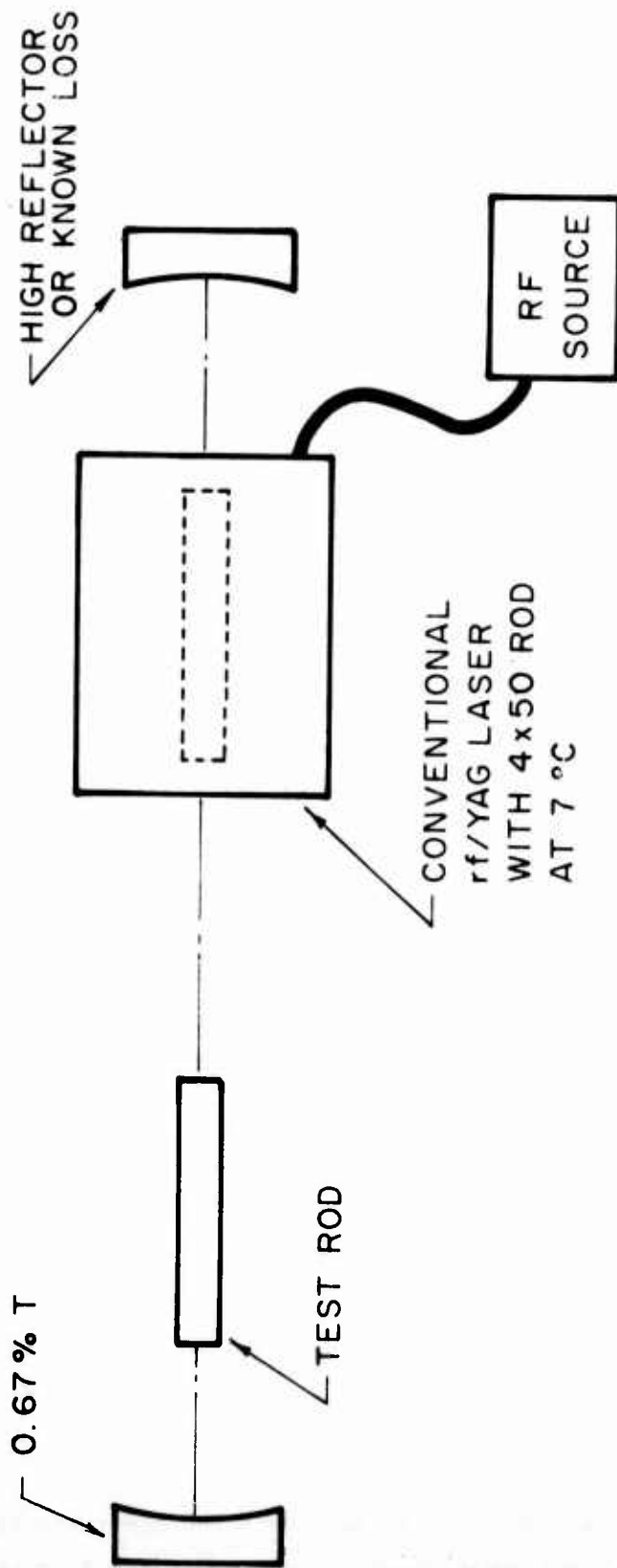


FIG. II ROD TEST SET-UP

## SECTION IV

### LASER PERFORMANCE

Several models of the side-pumped-laser were built and tested. The first, SPL-1, shown schematically in Figure 3, used the GFE 4x66mm rod discussed in Section III.5. The threshold and efficiency achieved with SPL-1 were both unprecedented for krypton pumping although performance was somewhat short of expectation. Much of the difficulty was associated with the relatively poor optical quality of the rod; however, it was also noted that considerable heat conduction was taking place from the lamp module to the rod heat sink.

With alternative laser rods being procured and mounted, a second model, SPL-2 was assembled. This model used a high quality rod and was assembled with the single goal of demonstrating acceptable efficiency in an SPL geometry. It successfully achieved this goal.

A third model, SPL-3, was designed to incorporate conductive cooling of a high quality rod. The test was unsuccessful. The reasons for the disappointing performance are numerous, and are discussed in detail below. None of them are pathological, and further experimentation should yield the desired result.

#### 1. Fabrication and Testing of SPL-1

Figure 3 is a schematic of SPL-1 and Figure 12 is a photograph of the structure with the coupling coil removed.

The lamp measured 14mm i.d., 16mm o.d. and 14mm long including a 6mm thick window. These dimensions were used in all subsequent models as well. The diffuse reflector was BaSO<sub>4</sub> paint.

Originally, SPL-1 was designed to pump only the central portion of the laser rod. The results were unsatisfactory; when operated in a resonator made up of two high reflecting mirrors the threshold rf power was 320 watts. The structure was modified to allow pumping over the entire length of the rod by including the side tubes shown in Figure 3. The threshold dropped to 195 watts.

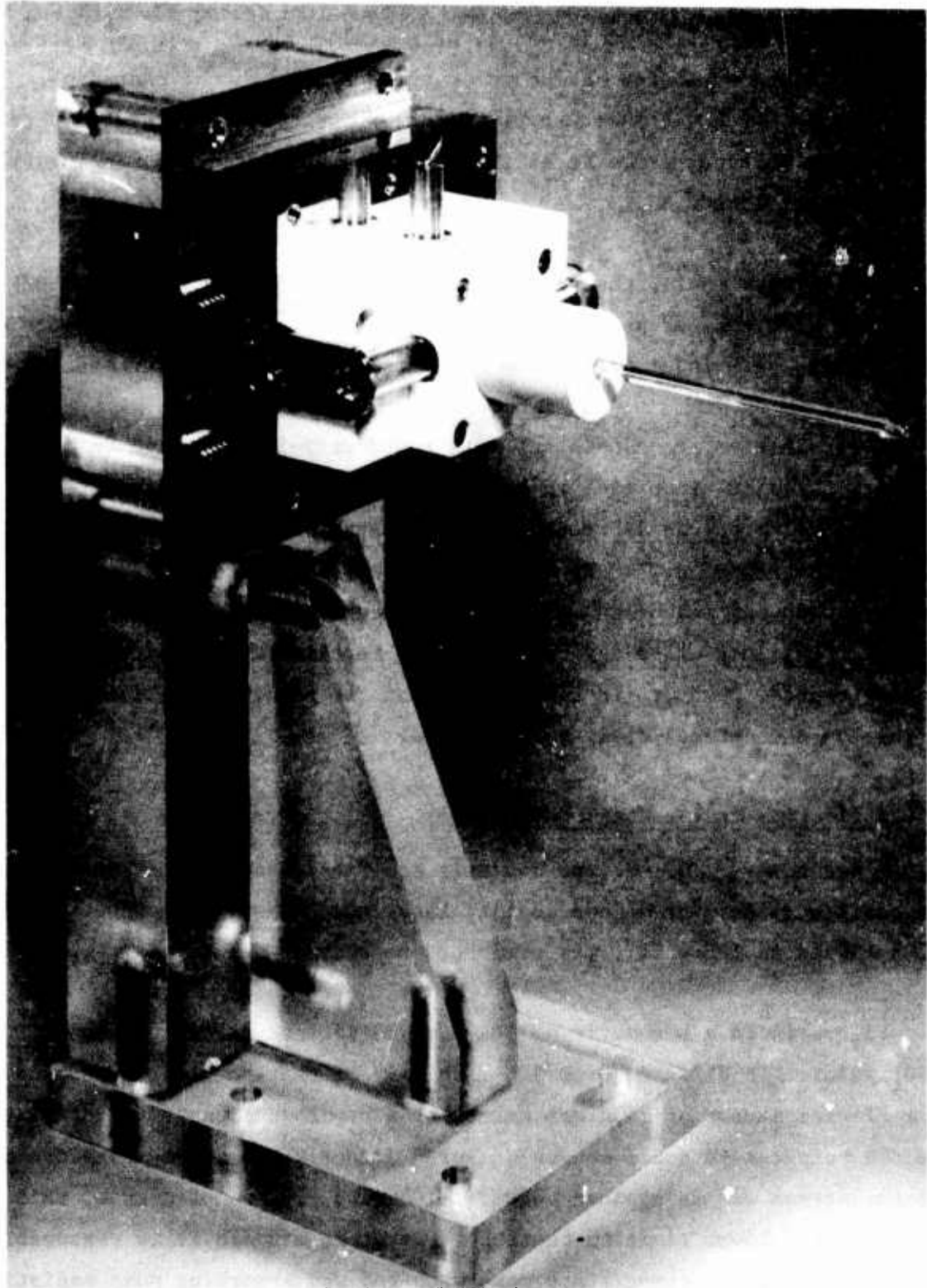


FIG 12 THE SPL-1

At this point, a second and final modification was made to SPL-1. Calculations indicated that a small gap between the rod and the diffuse reflector, indicated in Figure 13 should be the source of substantial optical loss. The gap was filled with diffuse reflecting paint, producing a marginal improvement; however, at this point, we postulated that heat generated in the lamp module was being conducted to the rod through the heat sink. Accordingly, we modified the power supply to allow long-pulse, quasi-cw operation. Experiments were performed at a 10Hz rate with pulse lengths ranging from one to five milliseconds.

At 10% duty cycle, the threshold dropped to 150 watts with two UHR mirrors. With a 1.67% transmitting mirror the threshold was 200 watts and at 250 watts peak input power, the multimode peak output power was 375 mw.

These results are consistent with round-trip-loss of five to six percent. A calculation made on the basis of the formalism presented in Section II predicts a threshold of 200 watts with a 1.7% transmitting mirror and a RTL of 6.2%. It further predicts a slope efficiency of 0.8% compared with the measured 0.75%. We feel constrained to point out, however, that such close agreement is to a certain extent fortuitous. We do feel secure, however, in concluding that the results were determined largely by the optical quality of the rod.

## 2. Fabrication and Testing of SPL-2

A second model, SPL-2, was designed and fabricated to test the basic SPL configuration with a good quality laser rod. The 4x50mm laser rod, No. 3 listed in Table III, was used for the tests.

Figure 14 is a schematic of SPL-2. The diffuse reflector was  $\text{BaSO}_4/\text{K}_2\text{SO}_4$  paint. It differed from SPL-1 chiefly in that the rod was cooled by a flowing stream of cold gas rather than by conduction to a heat sink. The rod temperature could not be measured directly but the temperature of the gas stream was maintained between  $-10^\circ\text{C}$  and  $-20^\circ\text{C}$ . Of course, this constitutes a lower limit to the rod temperature, though it is reasonable to believe that the temperature rose when rod was absorbing pump radiation.

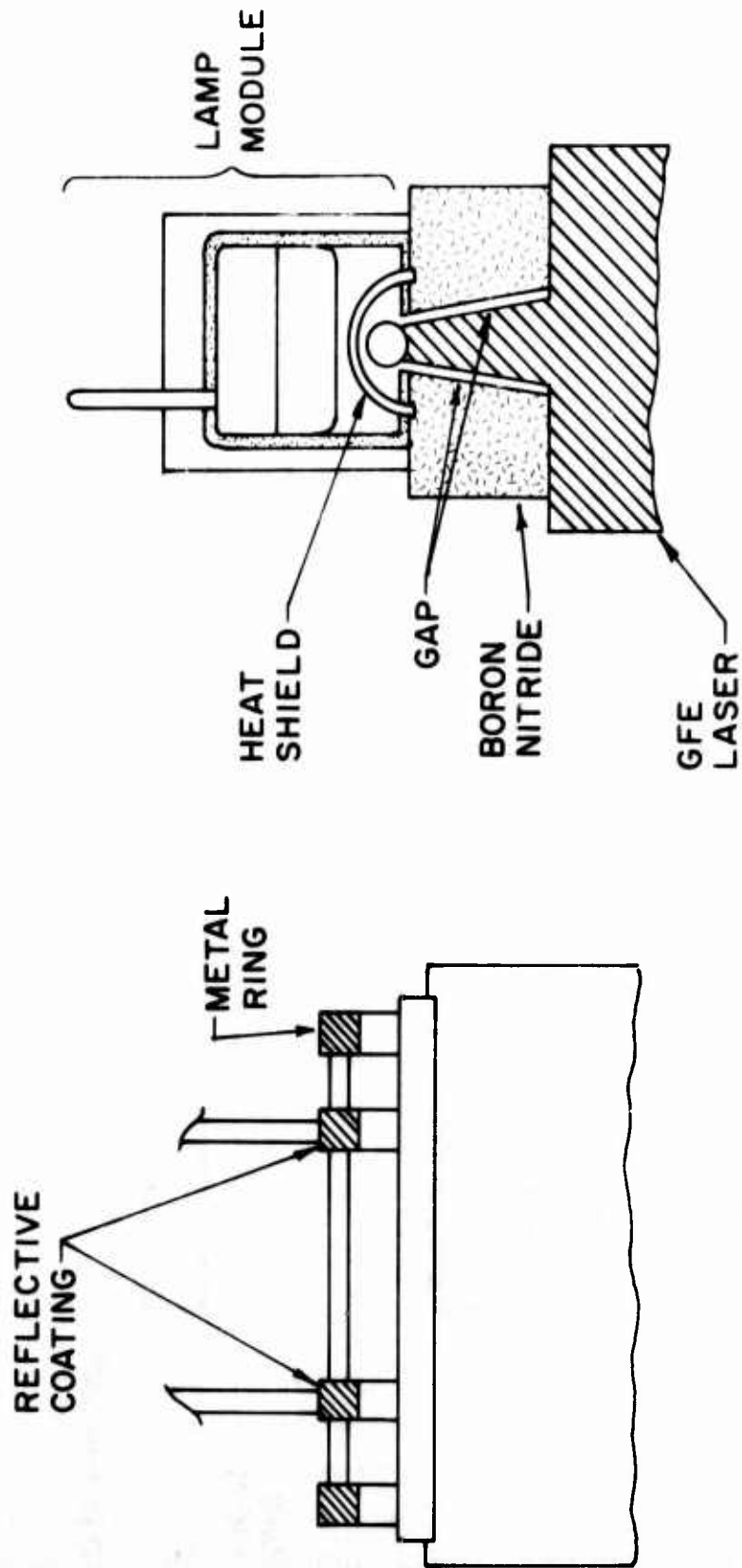
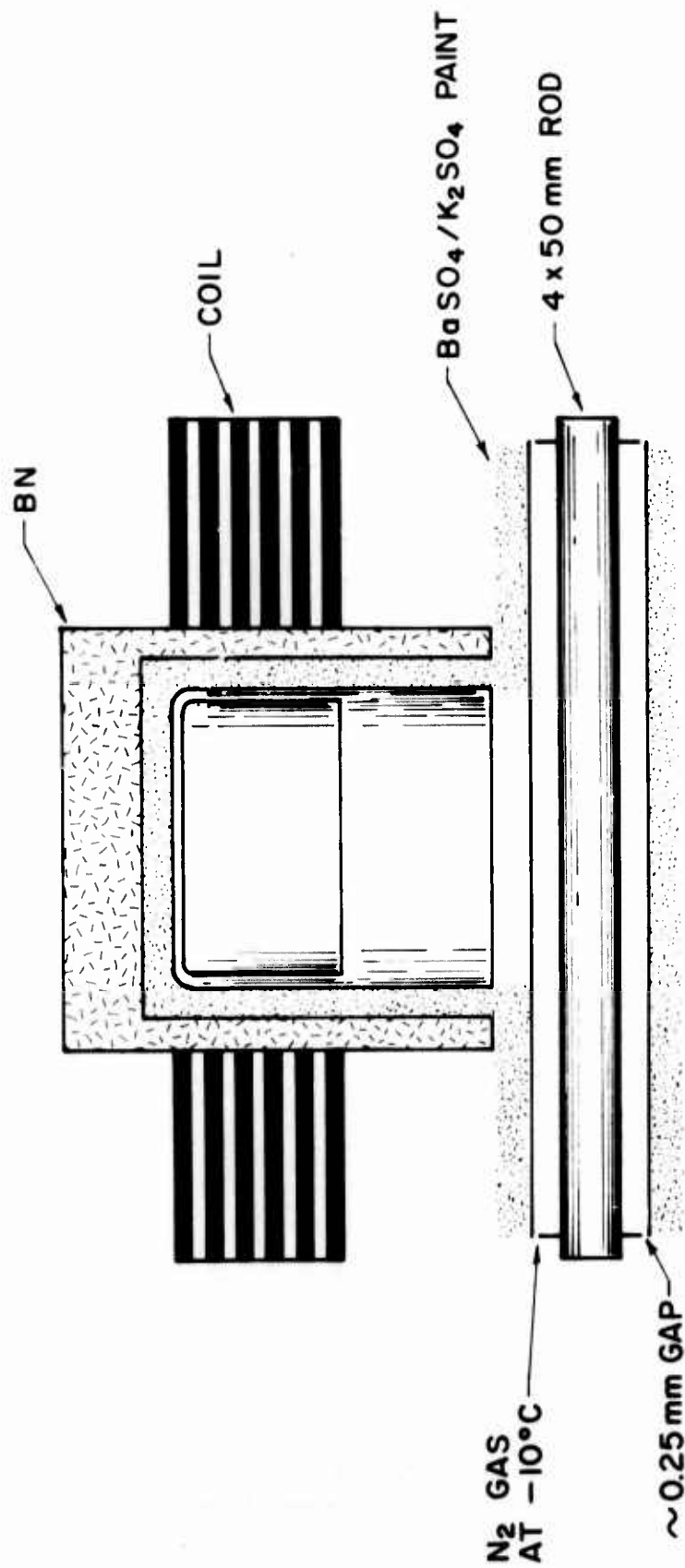


FIG. 13 DIAGRAM OF SPL-1



NITROGEN COOLED LASER

FIG. 14 SCHEMATIC OF SPL-2



Performance of SPL-2 in a 10% duty cycle mode is summarized in Figure 15. Both the threshold and slope efficiency improved dramatically over the results obtained with SPL-1. The threshold power required was 133 watts. The power output curve showed some curvature near threshold, however, in the straight line portion the slope efficiency was 1.5%. One watt of multimode output was observed for approximately 215 watts input. Reference to Figure 7 indicates good agreement for a laser rod with round-trip-loss of 3%.

The  $\text{BaSO}_4/\text{K}_2\text{SO}_4$  paint exhibits poor thermal conductivity which leads to overheating of the lamp. This issue is discussed in detail in Section V. An alternative diffuse reflector is Ceram LR-1 material which is an alumina-like ceramic. The thermal conductivity is quite high so that lamps in good contact with it will operate at moderate temperatures. The expectation was, however, that the optical efficiency would prove somewhat lower than for the paint.

Another model, SPL-2a, was built based upon a Ceram diffuse reflector around the lamp. Performance was slightly degraded. When tested with a 0.65% transmitting mirror at 10% duty cycle the threshold was 141 watts and the slope efficiency in the straight line portion of the curve was 1%. Our tentative conclusion was that the Ceram was indeed less efficient as a diffuse reflector than  $\text{BaSO}_4$ ; however, a gradual decrease in efficiency was observed throughout our studies on SPL-2 and 2a, an observation which we tentatively attribute to deterioration of the a-r coatings on the laser rod. The ultimate decrease in efficiency was of the order of 40%.

Model SPL-2a was also operated cw. With a low flow rate of cooling gas, the power output did not exceed 200 mw. When the flow rate was increased to a high level a cw output of 400 mw was achieved for 220 watts input. The pulsed and cw data are summarized in Figure 16. There is clear evidence of thermally induced saturation at high cw power levels.

The inability to accurately determine the laser rod temperature is, of course, an outstanding deficiency of SPL-2. However, below about  $-10^\circ\text{C}$ , rod temperature ceases to be an important parameter for pumping levels

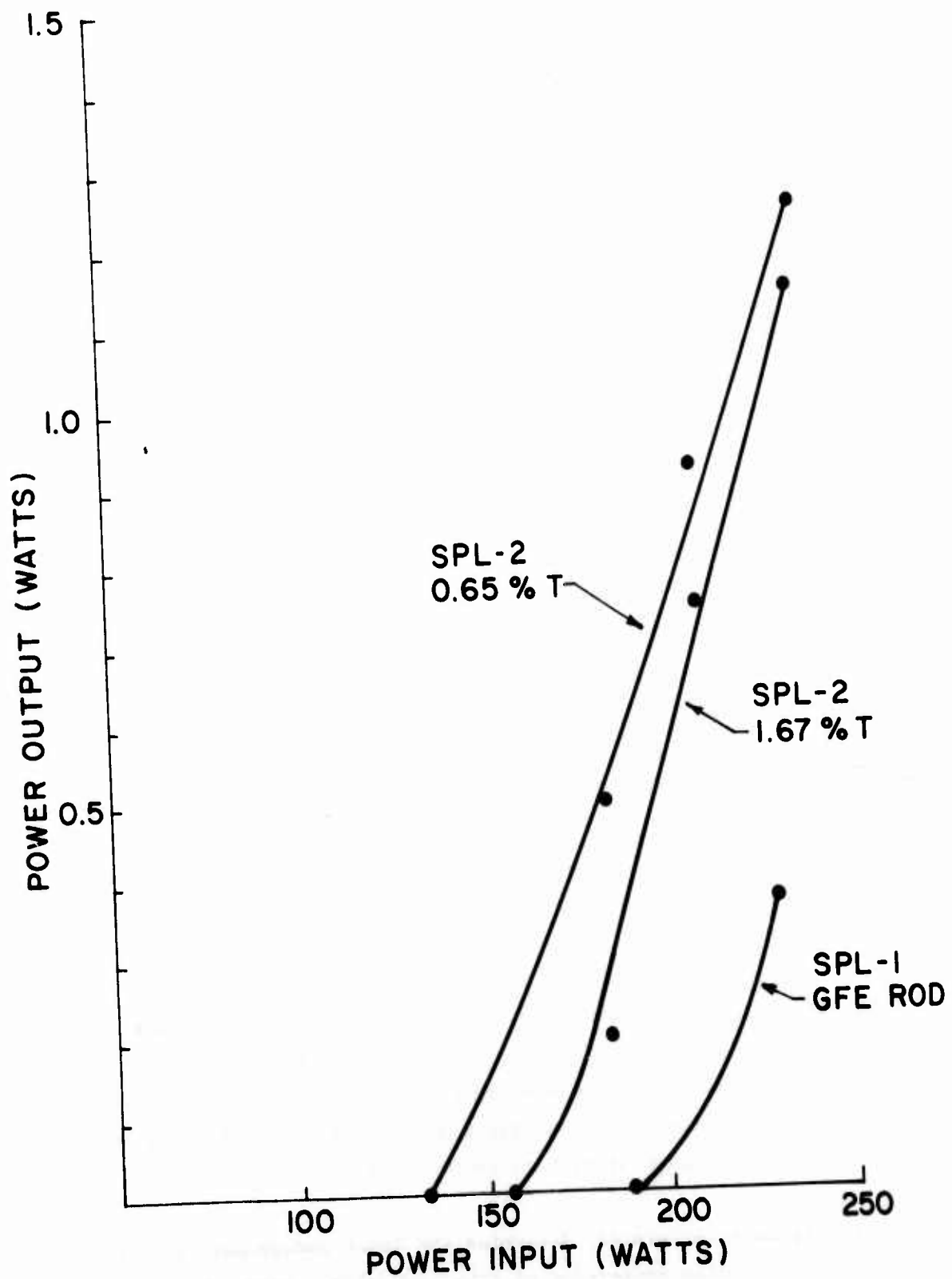


FIG. 15 PERFORMANCE OF SPL-2

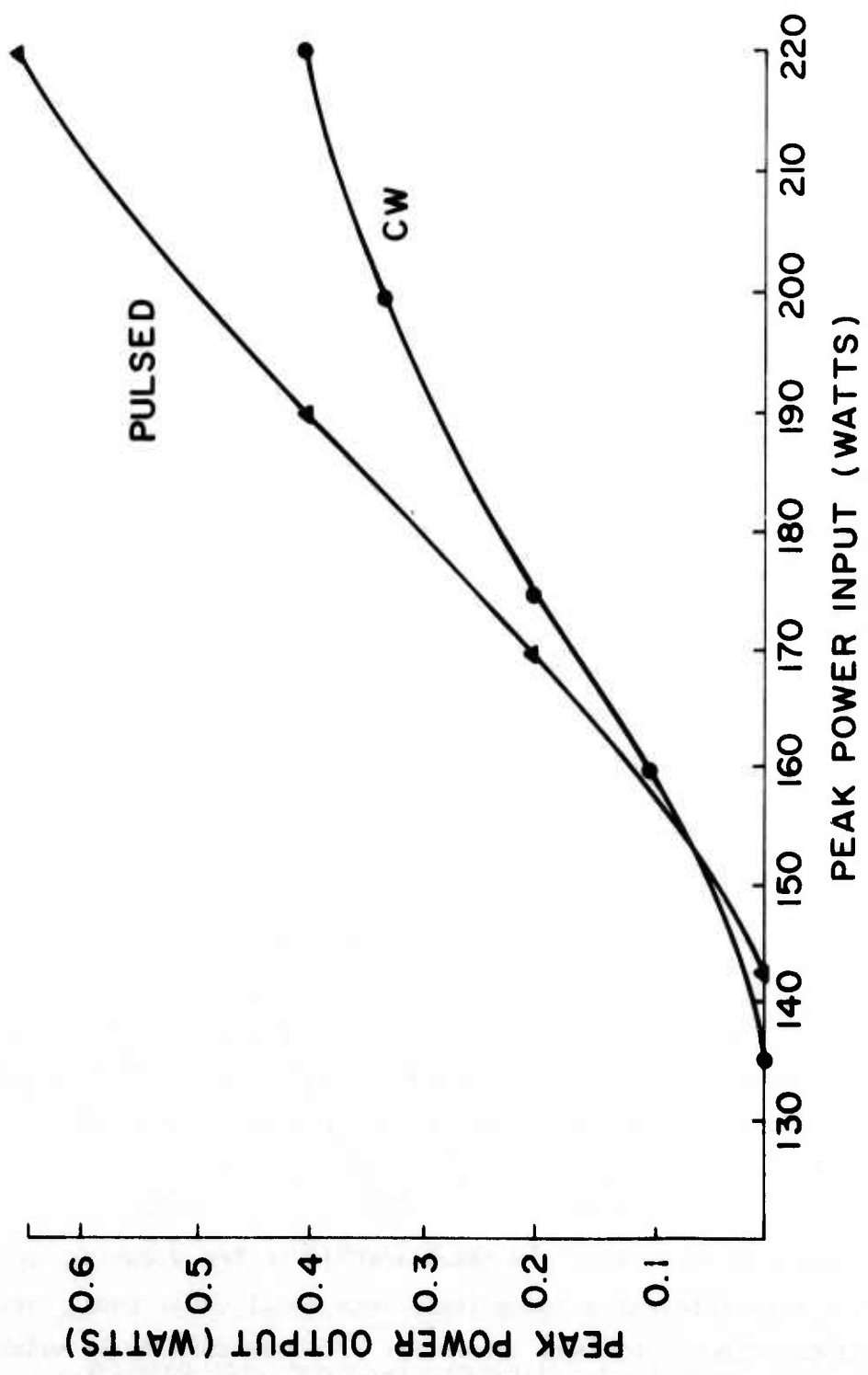


FIG 16 PERFORMANCE OF SPL-2a

above two or three times threshold. Reducing the rod temperature below  $-10^{\circ}\text{C}$  reduces the threshold power somewhat but to first order does not affect the slope efficiency. Figure 17 is a theoretical prediction of the power output from a nominal 1-watt laser as a function of rod temperature. It suggests that lowering the rod temperature from  $-10^{\circ}\text{C}$  to  $-30^{\circ}\text{C}$  will result in about a 20% increase in output power. Consequently, we believe that the question of the precise rod temperature in SPL-2 is not particularly important.

### 3. Fabrication and Assembly of SPL-3

A third model, SPL-3, was fabricated in an effort to combine the conductive cooling approach of SPL-1 with the high efficiency observed in SPL-2 and SPL-2a. Figures 18 and 19 are photographs of the assembled device.

Rod mounting and heat sinking techniques were beyond the original scope of this program, but were undertaken by Perkin-Elmer in the interest of testing SPL-3 as expeditiously as possible.

A fixture was fabricated to test the efficacy of various rod mounting techniques. The test rods were Pyrex cylinders measuring 3mm in diameter and 3cm long. The fixture consisted of two aluminum blocks each of which contacted the rod over about  $140^{\circ}$  of its periphery as shown in Figure 20. One block was heated electrically and the temperature difference across the rod was measured.

The contacting surfaces on the aluminum blocks were lapped and the rods were precision ground and polished. The grooves were usually wetted with a small amount of adhesive and a metal rod was pressed into it and rotated several times in an attempt to form a smooth, thin adhesive layer. Finally, the glass rod was placed in the groove and the adhesive was allowed to cool.

Table IV summarizes the results achieved for a variety of adhesives. Clearly, the differences among these were small under these circumstances. The Tra-Cast Epoxy 3011 was chosen for SPL-3 because it is soluble in

PREDICTED POWER OUTPUT  
vs. ROD TEMPERATURE

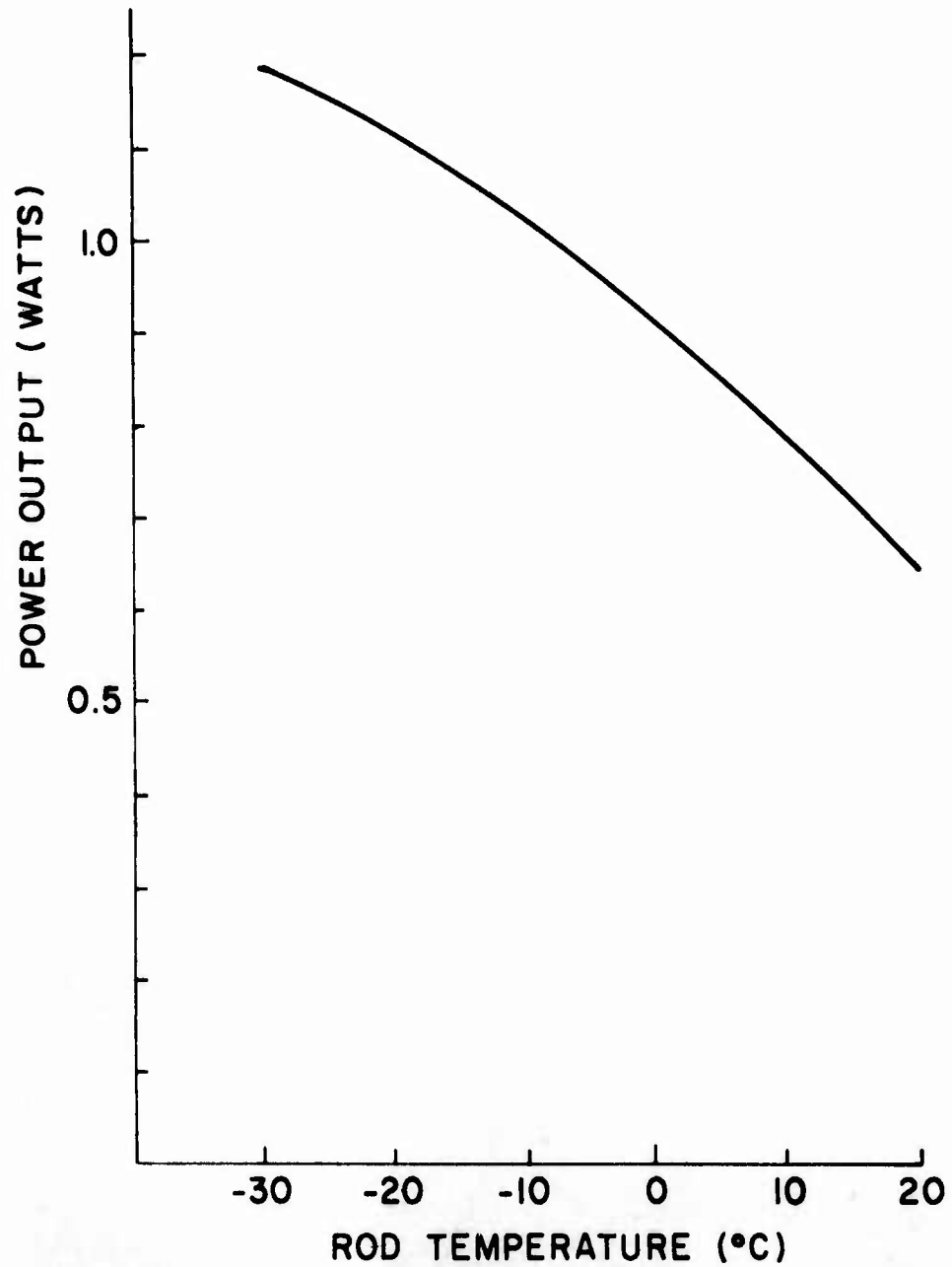


FIG. 17 PREDICTED POWER OUTPUT vs. ROD TEMPERATURE

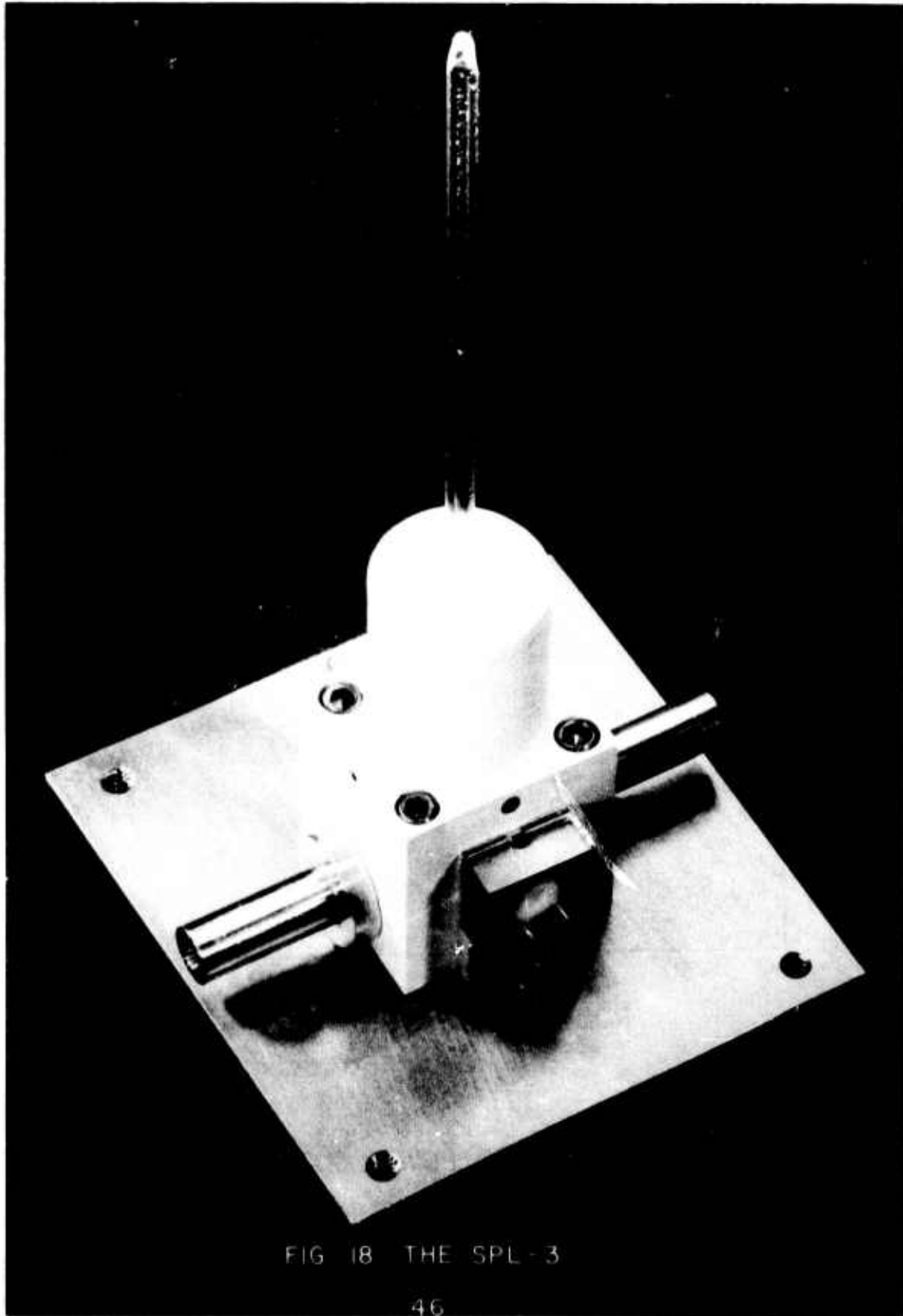


FIG 18 THE SPL-3

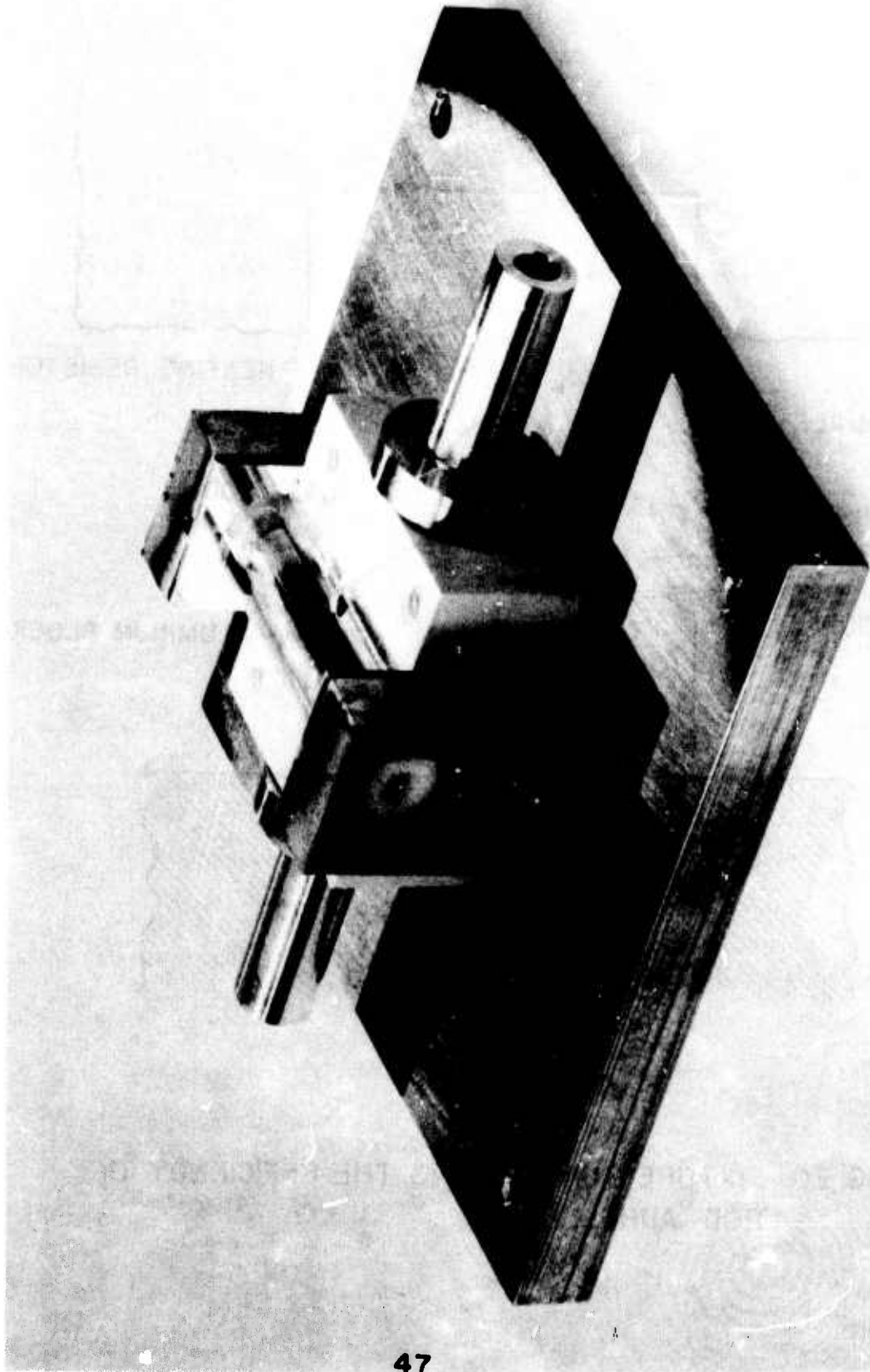


FIG. 19 INTERIOR OF SPL-3

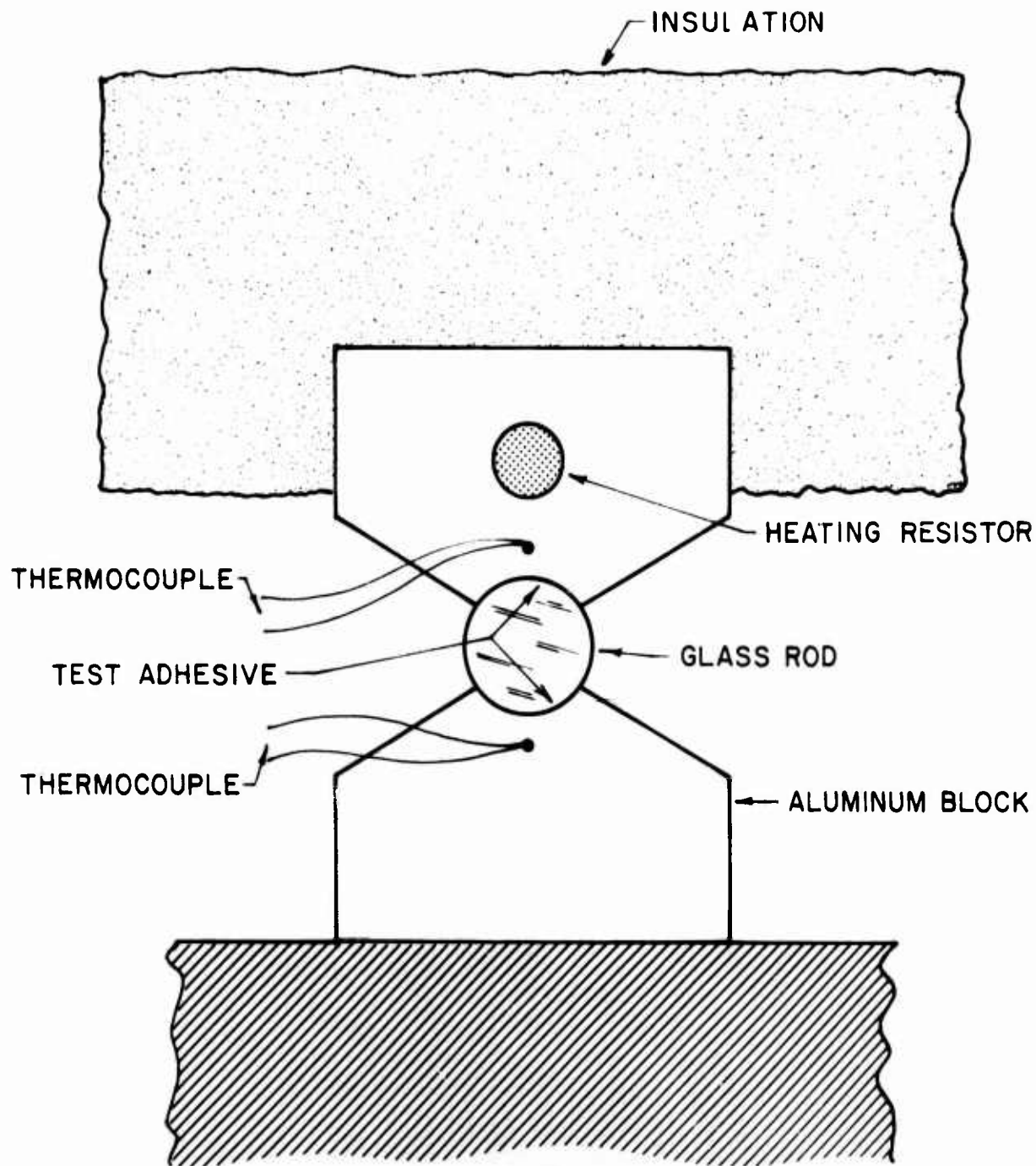


FIG. 20 FIXTURE FOR TESTING THE EFFICIENCY OF  
ROD ADHESIVES



TABLE IV

RESULTS OF ROD MOUNTING EXPERIMENTS

POWER INPUT TO RESISTOR = 2.45 WATTS

Adhesive	Temperature Difference Across Rod
GC Silicone 8109-S	20.5 °C
Tra-Cast Epoxy	21.75°C
GC Silver Paint	22.25°C
Metex TRV MA 509	23.4 °C
No adhesive	25 °C

methyl acetate and can consequently be readily removed.

The laser rod was mounted in the SPL-3 heat sink and the epoxy was allowed to cure at room temperature.

Model SPL-3 used the same lamp module as used for SPL-2; the optical coupling scheme is somewhat different as it incorporates a specularly reflecting surface in the immediate vicinity of the laser rod. This area, shown in Figure 21, was polished by single-point diamond machining. A layer of silver was deposited by rf sputtering followed by a rf sputtered silica protection layer.

Model SPL-3 was operated several times. The heat sink temperature was varied between 20°C and -30°C in the course of each experiment. Initially, it had a threshold of 150 watts and developed only 100 milliwatts peak output when pulsed to 250 watts peak at 10% duty cycle. In subsequent experiments, even this level of performance could not be duplicated. The disappointing behavior of SPL-3 can possibly be explained by the following observations.

- (i) One anti-reflection coating deteriorated badly due to thermal cycling. Figure 22 is a photograph of it.
- (ii) The rod was mechanically stressed by the heat sink as evidenced by the fact that laser beam reflections from the two faces were not parallel.
- (iii) The silver coating on the heat sink surface became tarnished in spite of the protective layer.

We suggest that the disappointing performance of SPL-3 can be explained in terms of these observations. Future work should concentrate on

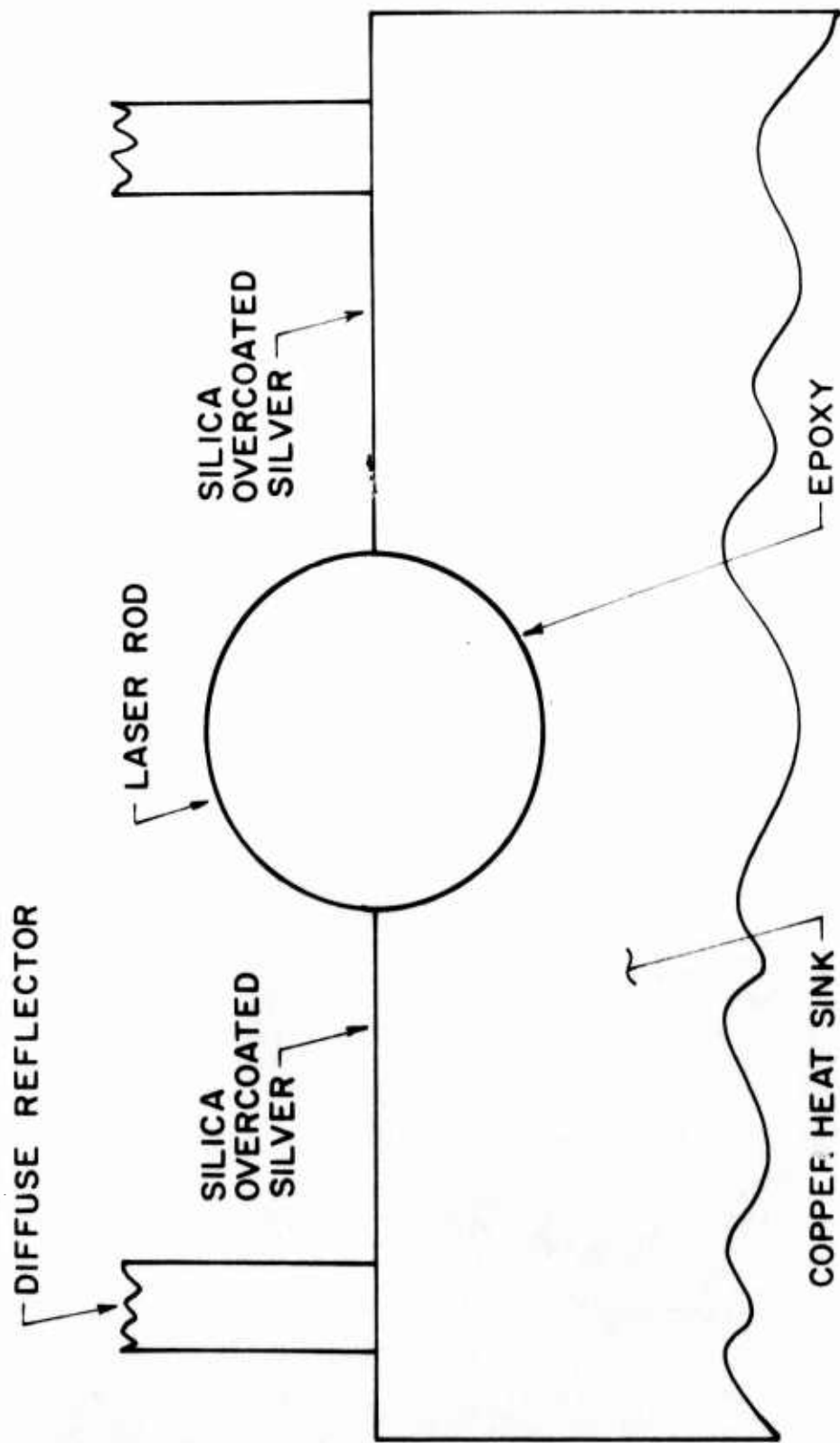


FIG. 21 THE SPL-3 IN THE VICINITY OF THE ROD



FIG. 22 ANTI-REFLECTION COATING ON LASER ROD  
FROM SPL-3

the following experiments and demonstrations:

- (i) Development of a strain-free rod bonding technique.
- (ii) Experimentation with different size rods.

## SECTION V

### LIFE TESTING

The electrodeless krypton arc lamp side-pumped laser design requires that the lamp be cooled by conduction through the diffuse reflector. This presents some difficulty, as the best reflector is  $\text{BaSO}_4/\text{K}_2\text{SO}_4$  paint, a very poor thermal conductor.

The original concept was to saturate the paint, which must be approximately 1mm thick, with helium gas. The conductivity of the combination was considered to be high enough to cool the lamp adequately. The approach was abandoned when we realized that the lamp operated at a sufficiently high temperature to allow the helium to diffuse in at a high rate.

The efficacy of the approach in cooling the lamp was easily demonstrated. A lamp was operated at 150 watts in a simple, 1mm-thick  $\text{BaSO}_4$  reflector. The envelope was clearly incandescent, indicating an operating temperature of approximately  $1200^\circ\text{C}$ . At this temperature, devitrification of the fused silica can be expected to develop at a high rate. However, the incandescence vanished as soon as the  $\text{BaSO}_4$  was saturated with helium.

We had previously observed that lamps operated in air showed no aging effects in 100 hours of operation. However, a lamp operated in  $\text{BaSO}_4/\text{He}$  showed a definite drop in output and increase in impedance after only 5 hours of operation. The drop in output could reasonably be associated with helium diffusing into the lamp through the hot fused silica. This phenomenon has been studied by Francis J. Norton<sup>(16)</sup> and based upon his data and an assumed operating temperature of  $500^\circ\text{C}$ , we calculated that the lamp could have contained 10% helium.

Additional evidence was obtained by baking the lamp in air to drive the helium out. After heating to  $700^\circ\text{C}$  for 16 hours, the lamp output returned to within 5% of its initial value.

A second experiment involving cooling through hydrogen was only

moderately more successful. Consequently, we discarded the concept of gaseous conduction cooling as any gas heavy enough not to diffuse through fused silica would not provide adequate cooling.

The alternative approach was to use high thermal conductivity diffuse reflectors such as Boron Nitride (BN), Ceram LR-1 or hot-pressed  $\text{BaSO}_4$ . The Ceram material, while readily available, was expected to exhibit somewhat lower reflectivity than  $\text{BaSO}_4$ . Our vendor for hot-pressed  $\text{BaSO}_4$  was Haselden Company of San Jose, California.

The next life test involved a lamp in fairly close proximity to a BN reflector. The gap between the lamp and the reflector was between .002 and .003 inch. The lamp was operated at 150 watts and the arc was extinguished approximately once every 24 hours and the structure was allowed to cool to room temperature before re-ignition. The minimum off-time was about an hour; the maximum was overnight.

The total lamp output was monitored continuously with an ILS power meter and the impedance was monitored by measuring the coil voltage. At the end of 1000 hours there was no discernable change in either output or impedance. The structure was disassembled and examined. Some devitrification of the envelope was observed, particularly in the center of the window which can be expected to be the hottest point in the structure.

Note that simple devitrification should not materially affect the coupling efficiency in a diffuse reflector since it merely introduces additional scattering. Any gases liberated as a result of the devitrification process were undetectable in either of the monitoring measurements.

But one is reluctant to extrapolate the present results to a 10,000-hour goal in the presence of devitrification. Consequently, a third life test is currently being performed. Figure 23 is a diagram of the arrangement. The test involves a lamp with a precision-ground outer diameter fitted into a diffuse reflector with a precision-ground inner diameter. The gap between the two is approximately 0.005 inch in the vicinity of the window. One can calculate that the window should be between 200°C and 300°C

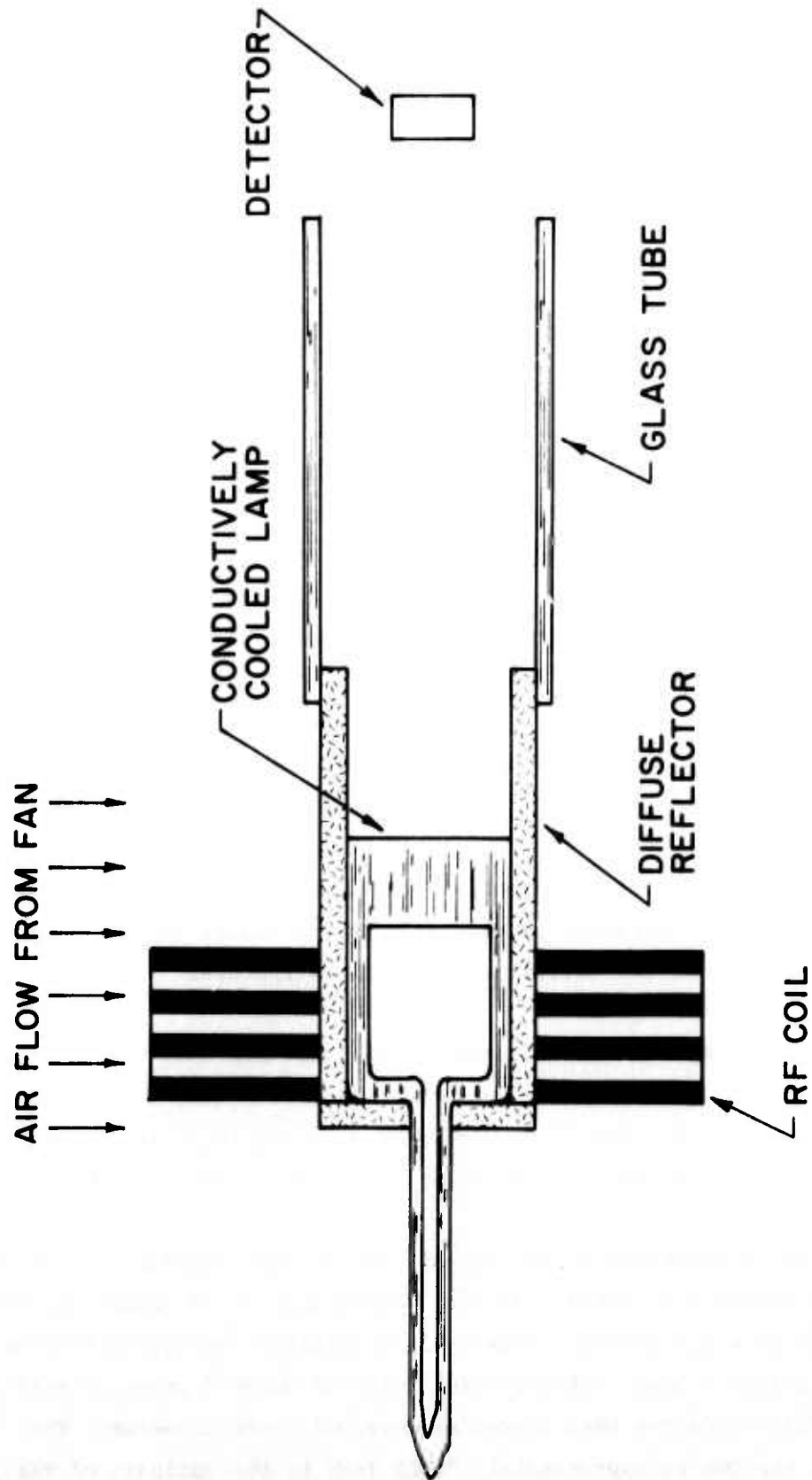


FIG. 23 LIFE TEST ARRANGEMENT



cooler in this case. The outside of the diffuse reflector is cooled to about 150°C by a fan. It would, of course, be possible to achieve a lower temperature but we felt that 150°C was a conservative approximation to the cooling that could be achieved in an all-conductive configuration. As of this writing, the test has passed the 270-hour mark. There is no appreciable change in total output.

The fabrication procedure for the precision lamps is illustrated in Figure 24.

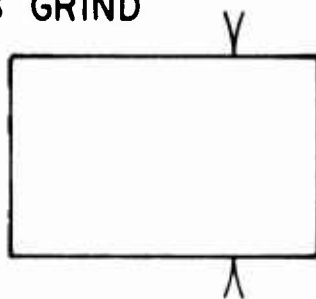
1. Solid fused silica rod was centerless ground to fit the diffuse reflector with a maximum gap of .004mm.
2. The plasma region was then core drilled.
3. The inside of the window was polished.
4. The back and pigtail were added by a glassblower.

Some slight shrinkage occurred during the final step which resulted in the gap increasing to .002 inch. However, calculations indicate that the temperature drop across the gap should be about 125°C and quite tolerable.

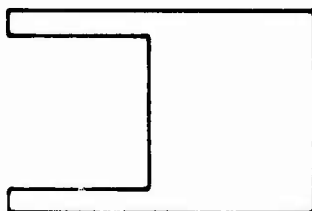
In retrospect, apparently the final grinding should have been performed after the back and pigtail were added, to avoid shrinkage. To be sure, the most critical part of the structure, the window, did not shrink. However, we will monitor the test closely and will examine the lamp carefully at the 1000-hour mark to see if the alternative procedure should be followed.

Additional monitoring procedures will be added to the 1000-hour test. The angular distribution of radiation will be checked at 1000-hour intervals to establish that subtle decreases in output are not taking place. In addition, the fraction radiation in the Nd:YAG pump band,  $\eta_2$  will be checked at similar intervals. This test was added to ensure that subtle changes in the spectral distribution would not go undetected. These changes will be correlated to the spectral outputs of the lamp and, in turn, of the laser as measured at zero lifetime.

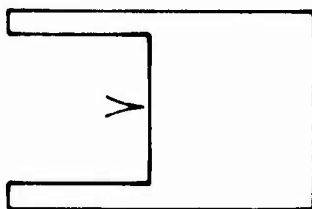
1. CENTERLESS GRIND



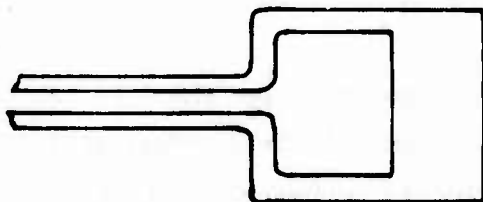
2. CORE DRILL



3. POLISH



4. ADD BACK, CUT OFF WINDOW



5. EXHAUST, BAKE OUT, FILL TO 2 atms.

FIG. 24 PRECISION LAMP FABRICATION

Our efforts to obtain samples of high conductivity  $\text{BaSO}_4$  were only partially successful. The vendor eventually delivered samples of flat discs which seem to exhibit conductivity similar to that of Ceram, however, he was unable to fabricate the cylindrical shape needed. Since the results on SPL-2 and SPL-2a were ambiguous on the question of whether  $\text{BaSO}_4$  was substantially more reflective than Ceram LR-1, the effort to procure appropriate  $\text{BaSO}_4$  samples was deferred.

## SECTION VI

### CONCLUSIONS AND RECOMMENDATIONS

This program addressed the question of the feasibility of pumping Nd:YAG with an electrodeless krypton arc lamp in a space environment. A special side-pumped configuration was proposed and evaluated, and an analysis of the power flow was developed in terms of a variety of threshold effects and coupling efficiencies. Two of the threshold parameters, the rf coil loss,  $P_c$ , and the lamp threshold power,  $P_{Lo}$ , are peculiar to the krypton electrodeless lamp. Under optimum conditions, the sum ( $P_c + P_{Lo}$ ) is 75 watts. This figure is substantially lower than the corresponding figure for dc krypton arc lamps for which Grasis and Reed<sup>(17)</sup> show a threshold of 270 watts for a 3mm-bore lamp. It is largely this difference which results in higher efficiency for electrodeless lamps, since this lamp radiation efficiency,  $\eta_1$ , and the fraction of the radiation falling in the pump band,  $\eta_2$ , are both similar to the performance measured by others for dc arc lamps.

The optical coupling efficiency,  $\eta_3$ , was assumed to be 70% in Section II. Values this high have been demonstrated in imaging ellipses. Further, we showed analytically in Section II and experimentally in Section III that  $\eta_3$  of 50% can be achieved in a diffuse reflector.

Clearly, the laser rod must be of good quality. A scattering and absorption loss of 0.2%/cm is quoted<sup>(18)</sup> as being characteristic of good material. Measurements described in Section III indicate that the value is indeed achieved in about half the laser rods tested. The heat-sink-mounted GFE laser rod furnished by the Air Force exhibited a round-trip-loss of approximately twice this value, that is, 6% or so. The power required to reach threshold is nearly proportional to the rod insertion loss and the slope efficiency is inversely proportional to it; thus a factor of two increase in RTL will decrease the overall efficiency very substantially.

The efficiency and power output of the first laser model, using the GFE rod, were consistent with our predictions. In detail, multimode peak

output power was 375 milliwatt for a rf input of 250 watts at a 10% duty cycle for a selected cavity mirror arrangement. The observed slope efficiency was 0.8%.

The basic efficiency questions were addressed in evaluating SPL-2 which used a dry nitrogen-cooled, good quality laser rod. The measured threshold and slope efficiency were in good agreement with the analytical model where the laser was operated in a long pulse mode. An output of 1 watt was achieved for 215 watts input and the measured slope efficiency was 1.5% with a round-trip-loss of 3%. However, rod heating effects were clearly apparent when the system was operated cw.

Model SPL-3 was based upon a good quality, heat-sink-mounted laser rod. Results were generally disappointing though it is reasonable to suggest that the reasons for the low output could be explained and that further experimentation should result in the demonstration of a cw device based upon a heat-sink-mounted rod which exhibits efficiency equal to or better than that observed with the SPL-2 model.

A 1000-hour life test of a conductively cooled lamp was successfully completed. The test included numerous on/off cycles. The arc was extinguished and re-ignited abruptly; no special care was taken to ensure slow temperature changes. There was some evidence of devitrification involving the hottest part of the envelope. However, there was no observable change in lamp output or impedance. A second life test was begun with a 5000-hour goal. The lamp is in closer contact with the heat sink, and we have calculated that it should run about 200°C cooler than the previous life test lamp. There has been no observable change in lamp performance after 200 hours.

Future work can concentrate in two areas. An optimized version of SPL-3 should be built. It should incorporate a good quality laser rod about 30mm long and possibly 4mm in diameter with optimized bonding to the heat sink. Further development of heat sinking techniques should concentrate upon the lamp modul including lamp, reflector and coil and a design compatible with heat-pipe cooling should be developed. Finally,

the relationship between lamp power and lamp life should be explored and a life test of a complete laser device should be performed.

Instead of using krypton gas fill for the lamp, the excitation of alkali-metal vapors by rf fields should also be explored. The advantage of alkali-metal pumping should be apparent in reduced lamp threshold. In the dc arc lamp case, the lamp threshold ( $P_{Lo}$  as distinct from the laser threshold  $P_{th}$ ) is roughly a factor of 5 lower for alkali metals than for krypton pumping. The overall efficiency may also improve because of a better spectral match to the absorption bands of Nd:YAG. The concept thus has the potential for developing a device with uniquely high efficiency with long life.

Core-drilled sapphire envelopes should be relatively free of thermally induced stresses. The use of polycrystalline envelopes rather than single crystal envelopes should also be explored. The scattering introduced by them should not have a significant effect in a diffuse reflector geometry.

#### REFERENCES

1. D.A. Huchital and G.N. Steinberg, Proc. IEEE, 60, 233 (1972).
2. D.A. Huchital, "RF-Excited Krypton Arc Lamps for Pumping Nd:YAG Lasers", AFAL-TR-74-135 (1974).
3. D.A. Huchital and G.N. Steinberg, IEEE J. Quant. Elect., QE-12, 1 (1976).
4. W. Koechner, Rev. Sci. Instr., 41, 1699 (1970).
5. Ibid.
6. J.D. Foster and L.M. Osterink, J. Appl. Phys. 41, 3656 (1970).
7. A.A. Shokin, Sov. J. Quant. Elect., 4, 238 (1974).
8. T. Kushida, H.M. Marcos and J.E. Geusic, Phys. Rev., 167, 289 (1968).
9. F.W. Ostermayer, Appl. Phys. Lett., 18, 93 (1971).
10. W.E. Thouret, Nat. Tech. Conf. of the Illuminating Eng'g. Soc., Sept. 7-11, 1959, San Francisco.
11. J. Whittle and D.R. Skinner, Appl. Optics, 5, 1179 (1966).
12. Op. Cit. 3
13. J.P. Charnoch and W.B. Jones, "Nd:YAG Mini-Face-Pumped Laser", AFAL-TR-73-446 (1973).
14. Op. Cit. 3
15. Op. Cit. 3
16. F.J. Norton, J. Appl. Phys. 28, 34, (1957).
17. M. Grasis and L. Reed, "Long Life Krypton Arc Lamps for Pumping Nd:YAG Lasers, AFAL-TR-73-156 (1973).
18. Op. Cit. 13